Structure−Activity Relationship of Synthetic Phosphoinositolglycans Mimicking Metabolic Insulin Action

Wendelin Frick, Andrea Bauer, Jochen Bauer, Susanne Wied, and Günter Müller*

Hoechst Marion Roussel Deutschland GmbH, Chemical and Metabolic Diseases Research Frankfurt, 65926 Frankfurt am Main, Germany

Received March 18, 1998; Revised Manuscript Received July 8, 1998

ABSTRACT: Phosphoinositolglycan (PIG) molecules have been implicated to stimulate glucose and lipid metabolism in insulin-sensitive cells and tissues in vitro and in vivo. The structural requirements for this partial insulin-mimetic activity remained unclear so far. For establishment of a first structure−activity relationship, a number of PIG compounds were synthesized consisting of the complete or shortened/mutated glycan moiety derived from the structure of the glycosylphosphatidylinositol (GPI) anchor of the GPI-anchored protein, Gce1p, from yeast. The PIG compounds were divided into four classes according to their insulin-mimetic activity in vitro with the typical representatives: compound **41**, HO-SO_2-O-6Manα1(Manα1-2)-2Manα1(6-HSO_3)-6Manα1-4GluNβ1-6(D)inositol-1,2-(cyclic)-phosphate; compound **37**, HO-PO(H)O-6Manα1(Manα1-2)-2Manα1-6Manα1-4GluNβ1-6(D)inositol-1,2-(cyclic)-phosphate; compound **7**, HO-PO(H)O-6Manα1-4GluN(1-6(L)inositol-1,2-(cyclic)-phosphate; and compound **1**, HO-PO-(H)O-6Manα1-4GluN(1-6(L)inositol. Compounds **41** and **37** stimulated lipogenesis up to 90% (at 20 μM) of the maximal insulin response but with differing concentrations required for 50% activation (EC_{50} values 2.5 ± 0.9 vs 4.9 ± 1.7 μM) as well as glycogen synthase (4.7 ± 1 vs 9.5 ± 1.5 μM) and glycerol-3-phosphate acyltransferase (3.5 ± 0.8 vs 8.0 ± 1.1 μM). Compound **7** was clearly less potent (20% of the maximal insulin response at 100 μM), whereas compound **1** was almost inactive. This relative ranking in the insulin-mimetic potency between members of the PIG classes (e.g., **41** > **37** ≫ **7** > **1**) was also observed for the (i) activation of glucose transport and glucose transporter isoform 4 translocation in isolated normal and insulin-resistant adipocytes, (ii) inhibition of lipolysis in adipocytes, (iii) stimulation of glucose transport and glycogen synthesis in isolated normal and insulin-resistant diaphragms, and (iv) induction of tyrosine phosphorylation of insulin receptor substrate-1 (IRS-1) in diaphragms. The complete glycan core structure (Man_3-GluN) of typical GPI anchors including a mannose side chain and the inositolphosphate moiety was required for maximal insulin-mimetic activity of the PIG compounds with some variations possible with respect to the type of residues coupled to the terminal mannose/inositol as well as the type of linkages involved. These data argue for the potency and specificity of the interaction of PIG molecules with putative signaling component(s) (presumably at the level of the IRS proteins) in adipose and muscle cells which finally lead to insulin-mimetic metabolic activity even in insulin-resistant states.

Insulin resistance occurs in a wide variety of pathological states and is a central component of non-insulin-dependent diabetes mellitus (for a review, see ref *1*). The frequent clustering of insulin resistance, hypertension, central obesity, hypertriglyceridemia, and accelerated atherosclerosis has led to the definition of a common metabolic condition often referred to as syndrome X (for a review, see ref *2*). Extensive efforts have been devoted to the identification of insulinomimetic agents that bypass the putative insulin resistance defect assumed to be located in one of the initial components of the insulin signaling cascade and that can stimulate glucose transport and metabolism in normal as well as insulin-resistant adipose and muscle cells. Introduction of nonhydrolyzable GTP analogues, muscle contraction/exercise, okadaic acid, anoxia, and osmotic shock can all stimulate glucose transport activity in isolated and cultured adipocytes or skeletal muscle cells (*3*−*8*). Furthermore, PIG[1] structures, the polar headgroups of a special class of glycolipids, free or protein-bound GPI lipids, have been demonstrated to modulate or even mimic metabolic insulin action to a certain degree (for a review, see ref *9*).

We recently prepared PIG molecules as PIG-P by sequential lipolytic and proteolytic digestion of the GPI anchor of Gce1p (*10*), which is a cell wall-associated cAMP-binding ectoprotein from the yeast *Saccharomyces cerevisiae* (*11*)

* Correspondence should be addressed to: Dr. Günter Müller, Hoechst Marion Roussel Deutschland GmbH, DG Metabolic Diseases Research, Bldg. H825, D-65926 Frankfurt am Main, Germany. Phone: ++4969-305-4271. Fax: ++4969-305-81767. E-mail: Guenter.Mueller@hmrag.com.

[1] Abbreviations: $EC_{20/50}$, effective concentration required for induction of 20/50% of the maximal insulin response; GLUT4, glucose transporter isoform 4; GPAT, glycerol-3-phosphate acyltransferase; GPI, glycosylphosphatidylinositol; GS, glycogen synthase; IRS-1, insulin receptor substrate-1; KRP, Krebs−Ringer phosphate buffer; MIR, maximal insulin response; PIG(-P), phosphoinositolglycan(-peptide); PMSF, phenylmethanesulfonyl fluoride; SDS−PAGE, sodium dodecyl sulfate polyacrylamide gel electrophoresis.

S0006-2960(98)00620-5 CCC: $15.00
Published on Web 08/29/1998

but during its biosynthesis transiently resides as a GPI-anchored protein at the plasma membrane (*12*). Interestingly, rat and 3T3-L1 adipocytes contain a similar cAMP-binding ectoprotein, the GPI anchor of which is lipolytically cleaved upon insulin challenge (*13*, *14*). The corresponding PIG-P is structurally completely defined and consists of the typical PIG structure identical for mammalian and yeast GPI-anchored proteins which is coupled via a phosphoethanolamine bridge and amide linkage to the tripeptide, NH_2-Tyr-Cys-Asn, derived from the carboxy-terminus of Gce1p. When assayed for insulin-mimetic activity in cellular systems, PIG-P stimulates lipogenesis in isolated rat adipocytes in a concentration-dependent manner up to 80% of MIR (at 10 μM) with EC_{50} values of 0.5−2 μM (*12*). Its activity is hardly reduced in cells which have been desensitized for insulin action either by proteolytic removal of the insulin receptor or by induction of insulin resistance during course of primary culture with high glucose and insulin concentrations. In addition, PIG-P exerts partial insulin-mimetic activity on a number of key metabolic pathways in rat adipocytes, cardiomyocytes, and diaphragms (*12*).

Since none of the insulin-mimetic stimuli mentioned above result in the activation of the insulin receptor kinase itself, it is anticipated that they converge with the insulin signaling pathway at a more distal step. With respect to PIG molecules, essentially no data are presently available concerning (i) the molecular target(s) and mechanism(s) of PIG action besides the apparent circumvention of the insulin receptor kinase and the use of IRS-1 and phosphatidylinositol 3-kinase (*15*) and (ii) the structural epitopes of the PIG molecules required for their activity. Such an analysis has been prohibited by the limited amounts as well as the heterogeneous and ill-defined structures of most of the various PIG preparations available from natural sources so far only.

As a first step in addressing these points, structural variants of the yeast PIG-P were synthesized. They contain either the complete or a less complex PIG portion but lack the peptide portion. Such a structural diversification can be achieved by chemical means only, since the core glycan of GPI-anchored proteins from which PIG-P has been derived is conserved during evolution from yeast to man (for reviews, see refs *16*−*18*). The partial and total syntheses of GPI structures, i.e., the GPI anchor of the variant surface glycoprotein from *Trypanosoma brucei* (*19*−*29*), the Thy-1 antigen from rat brain (*30*−*35*), and Gas1p from *S. cerevisiae* (*36*, *37*), or modified fragments of GPI anchors, e.g., (phospho)disaccharides (*38*−*43*), have been described previously, but in no case have significant and concentration-dependent biological effects exerted by these molecules in cellular or cell-free assay systems been documented in detail. As far as we know, the present study provides the first information on the insulin-mimetic activity of synthetic PIG compounds with regard to a variety of key metabolic enzymes and pathways in rat adipocytes and diaphragms leading to a preliminary structure−activity relationship.

MATERIALS AND METHODS

Materials. The sources of the animals and most of the materials and radiochemicals used have been described previously (*10*−*15*). All other materials were from Merck (Darmstadt, Germany) and of the highest purity available.

Synthesis of PIG Compounds

*Synthesis of Product **3** (Scheme 1, i)*. Product **1** (60 g, 94 mmol) (*35*) and 21.2 g (42.4 mmol) of product **2** (*44*) were dissolved in 200 mL of dry methylene chloride and 400 mL of dry *n*-heptane. After addition of 70 g of dried molecular sieves (0.4 nm), the mixture was stirred at room temperature for 15 min; 5 mL of 0.05 M trimethylsilyltrifluormethanesulfonic acid in methylene chloride (described as catalyst solution in the following procedures) was then added. After 15 min, 300 mL of *n*-heptane/ethyl acetate (1:1) was added, and the mixture was filtered through silica gel. The silica gel was washed with *n*-heptane/ethyl acetate (1:1), and the filtrate was then concentrated. After purification by means of flash chromatography, 41.0 g (99%) of **3** was obtained as a colorless oil. TLC: *n*-heptane/ethyl acetate (1:1), R_f = 0.6. MS: $(M + Li)^+$ = 981.1; calculated $C_{55}H_{67}N_3O_{11}Si$, M = 974.21.

*Synthesis of Product **4** (Scheme 1, ii, iii)*. Product **3** (41 g, 42.0 mmol) was dissolved in 400 mL of tetrahydrofuran (THF) and 9 mL of acetic acid. After addition of 70 mL of 1 M TBAF/THF solution, the mixture was allowed to stand at room temperature for 8 h. The acetic acid was removed by freezing (16 h at −30 °C), and the filtrate was purified by means of flash chromatography after concentration (yield 34.1 g = 94% of deprotected product). This was dissolved in 300 mL of dry methylene chloride. After addition of 50 mL of trichloroacetonitrile and 20 g of potassium carbonate, the mixture was stirred at room temperature for 4 h. It was filtered through silica gel, the silica gel was washed with *n*-heptane/ethyl acetate (1:1), and the filtrate was concentrated (crude yield: 42.1 g). TLC: *n*-heptane/ethyl acetate (2:1), R_f = 0.5. ^{1}H NMR ($CDCl_3$): characteristic signals for imidate; δ = 8.78, for NH and 5.63 for the anomer (β-imidate).

*Synthesis of Product **6** (Scheme 1, iv, v)*. Product **4** (33.2 g, 33.0 mmol) and 13.3 g (25.0 mmol) of product **5** (*45*, *46*) were dissolved in 120 mL of dry methylene chloride and 360 mL of dry *n*-heptane. After addition of 100 g of molecular sieves, the mixture was stirred at room temperature for 15 min. It was cooled to −20 °C under argon and then treated with 20 mL of catalyst solution. After 30 min, the mixture was allowed to thaw to room temperature. For workup, it was filtered through silica gel, and the silica gel was washed with *n*-heptane/ethyl acetate (1:1). The filtrate was concentrated, and the crude product (46.2 g) was dissolved in 150 mL of methylene chloride. After addition of 400 mL of methanol and 15 mL of 1 M NaOMe/MeOH solution, the mixture was allowed to stand at room temperature for 16 h. The solution was treated with 1 mL of water and concentrated. The oil obtained was dissolved in 50 mL of ethyl acetate, diluted with 200 mL of *n*-heptane/ethyl acetate (1:1), and filtered through silica gel. After concentration, the residue was purified by flash chromatography (yield 32.5 g = 97% of white foam as an anomer mixture). TLC: *n*-heptane/ethyl acetate (2:1), R_f = 0.5. MS: $(M + Li)^+$ = 1336.7; calculated $C_{80}H_{87}N_3O_{15}$, M = 1330.59.

*Synthesis of Product **7** (Scheme 1, vi, vii)*. The anomer mixture of product **6** could only be easily separated chromatographically as the product **7**; 32.4 g (24.4 mmol) of product **6** was dissolved in 200 mL of methylene chloride. After addition of 500 mL of 0.5 M HCl/MeOH (from 17.5

Scheme 1: Strategy for the Chemical Synthesis of PIG Compounds[a]

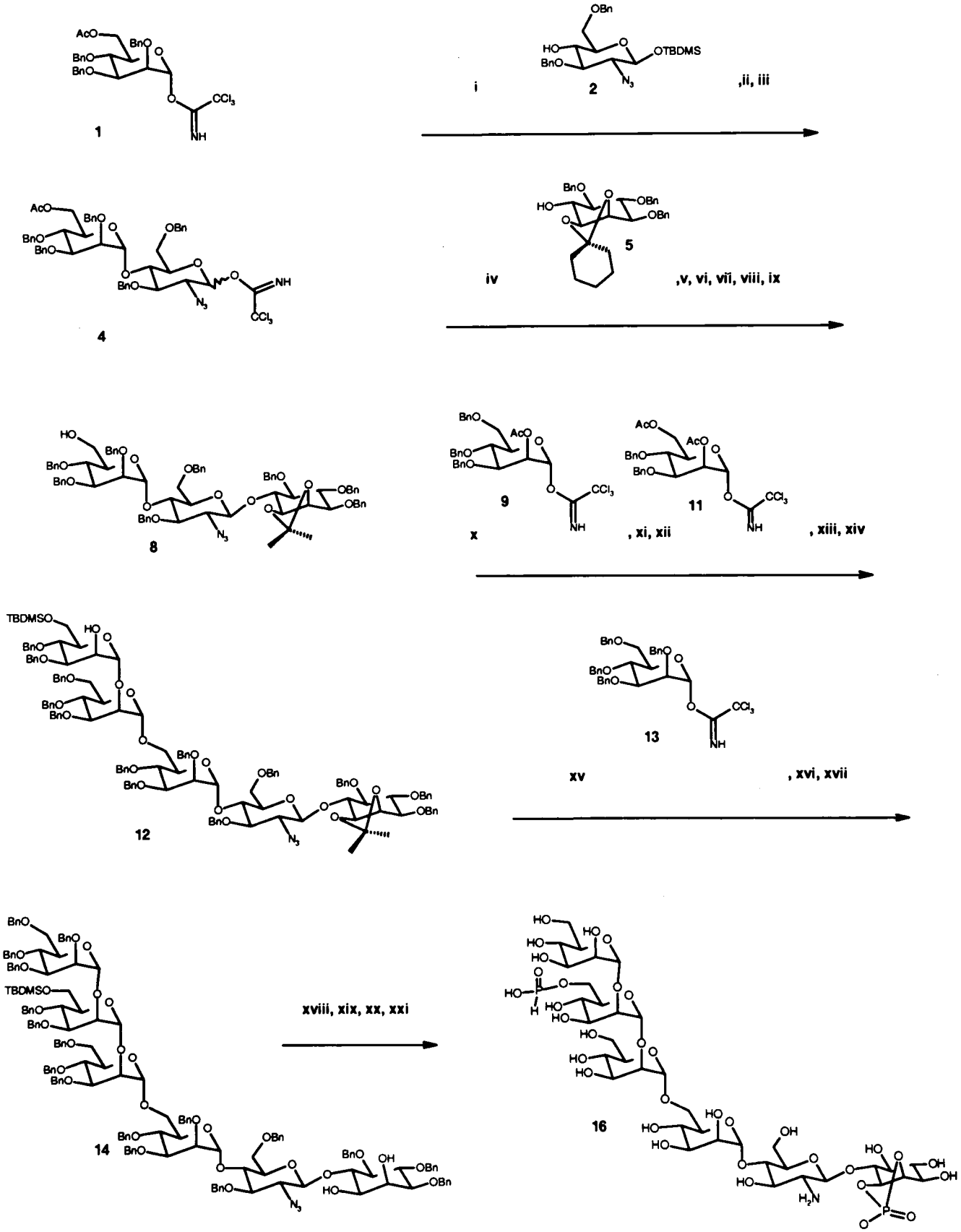

[a] (i) **2**/TMS−Trf/4 Å molecular sieves, 99% crude product; (ii) TBAF/AcOH $\mathbf{2}_{aq}$/THF, 94%; (iii) Cl_3CCN/K_2CO_3, 99% crude product; (iv) **4**/TMS−Trf/4 Å molecular sieves; (v) NaOMe; (vi) HCl/MeOH; (vii) TBDMSCl, imidazole; (viii) dimethoxypropane, TsOH; (ix) TBAF, 61% β and 19% α from products **3**−**5**; (x) **6**/TMS−Trf/4 Å molecular sieves; (xi) NaOMe, 76% from product **5**; (xii) **7**/TMS−Trf/4 Å molecular sieves; (xiii) NaOMe; (xiv) TBDMSCl/imidazole, 95% over three steps; (xv) **9**/TMS−Trf/4 Å molecular sieves; (xvi) HCl/MeOH; (xvii) TBDMSCl, imidazole, 84% over three steps; (xviii) tris(1,2,4-triazolyl)phosphate, 97%; (xix) TBAF, 99%; (xx) $P(OH)_3$/PivCl, 91%; (xxi) $NaNH_3(I)$, NH_4Cl, 78% from product **16** which corresponds to compound **37**.

mL of AcCl in 500 mL of MeOH) and 20 mL of ethylene glycol, the mixture was allowed to stand at room temperature for 17 h. After concentration, the residue was purified by flash chromatography. The product obtained (26.9 g, 88%) was dissolved in 300 mL of methylene chloride; 3.0 g of imidazole and 4.6 g of TBDMSCl were added. After 16 h at room temperature, the mixture was diluted with 500 mL of *n*-heptane/ethyl acetate (2:1) and filtered through silica gel. The silica gel was washed with *n*-heptane/ethyl acetate (2:1), and the filtrate was concentrated. The crude product obtained was purified by flash chromatography [yield 21.1 g = 72% of product **7** and 6.3 g (22%) of α-product]. TLC: *n*-heptane/ethyl acetate (2:1), $R_f = 0.5$ for **7** and $R_f = 0.3$ for the α-product. MS: $(M + Li)^+ = 1370.6$; calculated $C_{80}H_{93}N_3O_{15}Si$, M = 1364.71.

*Synthesis of Product **8** (Scheme 1, viii, ix).* Product **7** (21.2 g, 15.5 mmol) was dissolved in 60 mL of methylene chloride and 180 mL of dimethoxypropane; 250 mg of TsOH was added, and the mixture was allowed to stand at room temperature for 1 h. After addition of 2 mL of triethylamine, it was concentrated and 23.1 g of crude product was obtained. This was dissolved in 150 mL of THF and treated with 30 mL of 1 M TBAF/THF solution. After 16 h, it was concentrated and purified by flash chromatography (yield 20.0 g = 99% of product **8** as a white foam). TLC: *n*-heptane/ethyl acetate (2:1), $R_f = 0.4$. MS: $(M + Li)^+ = 1296.7$; calculated $C_{77}H_{83}N_3O_{15}$, M = 1290.51.

*Synthesis of Product **10** (Scheme 1, x, xi).* Product **8** (20.0 g, 15.4 mmol) and 15.0 g (23.5 mmol) of product **9** (*36*) were reacted analogously to the procedure for product **6**, and 20.3 g (76%) of product **10** was obtained as a white foam. TLC: *n*-heptane/ethyl acetate (2:1), $R_f = 0.6$. MS: $(M + Li)^+ = 1770$, calculated $C_{107}H_{115}N_3O_{20}$, M = 1763.09.

*Synthesis of Product **12** (Scheme 1, xii, xiii, xiv).* Product **10** (20.3 g, 11.8 mmol) and 12.0 g (20.3 mmol) of product **11** (*36*) were reacted analogously to the procedure for product **6**, and 19.4 g (80%) of deacylated product was obtained. This product was dissolved in 200 mL of methylene chloride and treated with 3.4 g (50.0 mmol) of imidazole; 6.0 g (40.0 mmol) of TBDMSCl was added, and the mixture was stirred at room temperature for 15 h. After addition of 5 mL of methanol, it was allowed to stand for 10 min, then diluted with 200 mL of *n*-heptane/ethyl acetate (1:1), and filtered through silica gel. The silica gel was additionally washed with 200 mL of *n*-heptane/ethyl acetate (1:1), and the filtrate was concentrated and purified by means of flash chromatography (yield: 19.4 g = 95% of product **12** as a white foam). TLC: *n*-heptane/ethyl acetate (2:1), $R_f = 0.7$. MS: $(M + Li)^+ = 2226$; calculated $C_{133}H_{151}N_3O_{25}Si$, M = 2219.75.

*Synthesis of Product **14** (Scheme 1, xv, xvi, xvii).* Product **12** (19.4 g, 8.9 mmol) and 14.0 g (20.0 mmol) of product **13** (*36*) were dissolved in 100 mL of dry methylene chloride and 300 mL of dry *n*-heptane. After addition of 40 g of molecular sieves (0.4 nm), the mixture was stirred at room temperature for 15 min; 10 mL of catalyst solution was added, and the mixture was stirred for a further 15 min. For workup, it was filtered through silica gel and the silica gel was washed with *n*-heptane/ethyl acetate (1:1). The filtrate was concentrated, and 33 g of crude product was obtained. This was dissolved in 200 mL of methylene chloride and treated with 500 mL of 0.5 M HCl in methanol. After 2 h at room temperature, the mixture was concentrated several times with methylene chloride. The intermediate obtained was dissolved in 200 mL of methylene chloride and treated with 3.4 g (50 mmol) of imidazole and 6.0 g of (40 mmol) of TBDMSCl. After 16 h, the mixture was worked up analogously to product **12** (yield 20.2 g = 85% of product **14** as a white foam). TLC: *n*-heptane/ethyl acetate (2:1), $R_f = 0.3$. MS: $(M + Li)^+ = 2669$; calculated $C_{161}H_{177}N_3O_{30}Si$, M = 2662.26.

*Synthesis of Product **15** (Scheme 1, xviii, xix).* Triazole (30.0 g) was dissolved in 800 mL of dry THF; 13.5 mL of phosphorus oxychloride was added dropwise at 10 °C; 60 mL of triethylamine was then added dropwise, and the mixture was stirred at room temperature for 15 min. The precipitate was filtered and washed with a little dry THF. The filtrate was added to 19.1 g (7.2 mmol) of product **14**. The solution was concentrated to 100 mL. After 15 min, it was diluted with 500 mL of ethyl acetate and washed twice with 100 mL of water. The organic phase was dried over magnesium sulfate, filtered, and concentrated. After flash chromatography, 19.0 g (97%) of cyclic phosphate derivative was obtained as a white foam. TLC: methylene chloride/methanol/33% NH_3 (100:7:1), $R_f = 0.3$. MS: $(M + 2Li - H)^+ = 2737$; calculated $C_{161}H_{174}N_3O_{32}PSi$, M = 2724.22. The cyclic phosphate was dissolved in 350 mL of THF, and 100 mL of TBAF (1 M in THF) was added. After 20 h, the mixture was concentrated and the residue was purified by flash chromatography (yield 18.1 g = 99% of product **15** as a white foam). TLC: methylene chloride/methanol/33% NH_3 (100:7:1), $R_f = 0.3$ (runs identically to the starting material). MS: $(M + 2Li - H)^+ = 2622$; calculated $C_{155}H_{162}N_3O_{32}P$, M = 2609.96.

*Synthesis of Product **16** (Scheme 1, xx, xxi).* Phosphorous acid (14 g) was concentrated four times with pyridine and then taken up in 200 mL of dry pyridine; 16 mL of pivaloyl chloride was added dropwise at 10 °C. This reaction solution was allowed to stand at room temperature for 15 min; 18.1 g (6.9 mmol) of product **15** was introduced into the reaction solution as described above. After 1 h, it was diluted with 200 mL of toluene and 150 mL of methylene chloride/methanol/33% NH_3 (30:10:3). After concentrating, residual pyridine was distilled out a further three times with toluene. The residue was suspended in 200 mL of methylene chloride/methanol (20:1). The nonsoluble constituents were filtered and washed twice with 50 mL of methylene chloride/methanol (20:1). The filtrate was concentrated and purified by flash chromatography (yield 16.9 g = 91% of protected final product). TLC: methylene chloride/methanol/33% NH_3 (100:7:1), $R_f = 0.25$. MS: $(M + 3Li - 2H)^+ = 2691$; calculated $C_{155}H_{163}N_3O_{34}P_2$, M = 2673.94. For deprotection, 600 mL of ammonia was condensed at −78 °C; 4.7 g (204 mmol) of sodium was dissolved therein. This solution was diluted with 300 mL of dry THF, and 16.9 g (6.3 mmol) of protected final product dissolved in 100 mL of dry THF was then slowly added dropwise at a reaction temperature of −78 °C. After a reaction time of 15 min (blue color must not disappear), the mixture was treated cautiously with 10 g of ammonium chloride. When the blue color had disappeared, the mixture was diluted cautiously with 100 mL of water and 300 mL of methanol. It was allowed to thaw and then concentrated to around 150 mL. This solution was diluted with 2 mL of methylene chloride/methanol/33% NH_3 (3:3:

1) and added to a flash silica gel column (700 mL of silica gel). It was eluted with 3 L of methylene chloride/methanol/33% NH_3 (3:3:2) and then with 3 L of methylene chloride/methanol/33% NH_3 (3:3.5:3). The product eluted was then chromatographed using *n*-butanol/ethanol/water/33% NH_3 (2:2:2:1) (yield 5.5 g = 78% of product **16** as a white solid). TLC: (2:2:2:1), $R_f = 0.4$. MS: $(M + H)^+ = 1116.5$; calculated $C_{36}H_{63}NO_{34}P_2$, M = 1115.83. ^{31}P NMR (D_2O) $\delta = 16.3$ ppm for cyclic phosphate and 7.9 for H-phosphate.

Preparation and Incubation of Rat Adipocytes. Rat adipocytes were obtained by collagenase digestion of epididymal fat pads from male Wistar rats (140−160 g) (unless indicated otherwise) or Zucker fatty rats (350−400 g) as described previously (*47*, *48*) and finally washed and suspended at the cell titer indicated in KRP−Hepes buffer (25 mM Hepes free acid, 25 mM Hepes sodium salt, 130 mM NaCl, 1.4 mM $MgSO_4$, 2 mM $CaCl_2$, 6 mM KCl, 10 mM KH_2PO_4, 1 mM sodium pyruvate, 1% BSA, pH 7.4, bubbled with 95% O_2/5% CO_2) containing glucose as appropriate for the subsequent assays (see below). For desensitization of adipocytes toward insulin action, rat adipocytes were incubated in Hepes-buffered salt solution containing either 5 mM glucose (control cells) or 20 mM glucose, 16 mM glutamine, 10 nM insulin (desensitized cells) for 16−20 h at 37 °C and further processed as described previously (*49*). For proteolytic removal of the insulin receptor, rat adipocytes were incubated with 40 μg/mL trypsin (trypsinized cells) or trypsin plus a 4-fold molar excess of bovine trypsin inhibitor (control cells) for 20 min at 37 °C and further processed as described recently (*12*). Control and treated adipocytes were handled in identical manner during the subsequent washing and flotation cycles. Isolated and washed rat adipocytes were incubated with PIG compound or insulin in KRP−Hepes buffer (3.5×10^5 cells/mL) containing 0.1 mM glucose for 20 min at 37 °C under constant mild shaking in a water bath and continuous bubbling with 95% O_2/5% CO_2.

Preparation and Incubation of Rat Diaphragms. Intact diaphragms (with rib cage attached) were dissected from male Wistar rats (60−80 g, fed ad libitum) or Zucker fatty rats (110−130 g) killed by cervical dislocation as described previously (*15*) and washed once with saline and once with KRO buffer (140 mM NaCl, 6 mM KCl, 2 mM $CaCl_2$, 1 mM $MgSO_4$, 1.2 mM KH_2PO_4, 0.1% BSA, 25 mM Hepes/KOH, pH 7.5, equilibrated with O_2) containing 5 mM glucose. The diaphragms were then dissected into halves (hemidiaphragms) and incubated in 20 mL, each, of KRO buffer containing 5 mM glucose for 30 min at 30 °C under continuous bubbling with 95% O_2/5% CO_2, followed by two 15-min periods of incubation in the presence of insulin/PIG compound with fresh buffer, each, under the same conditions. Subsequently, the diaphragms were washed with KRO buffer containing 2 mM pyruvate and 5 mM sucrose.

Assays for Insulin-Mimetic Activity. Lipogenesis was measured as incorporation of glucose into toluene-extractable lipids after addition of [3-^{3}H]glucose (0.4 μCi) to the adipocyte suspension adjusted to 140 M (low glucose) or 2 mM (high glucose) total final glucose concentration as described previously (*48*) and incubation for 90 min at 37 °C. GPAT activity was determined as incorporation of [^{3}H]-glycerol-3-phosphate (0.5 μCi, 0.2 mM final concentration) into butanol-extractable lipids using a crude microsomal fraction (150000*g*/60 min pellet of a defatted postmitochondrial fraction from rat adipocytes) during incubation with 150 μM palmitoyl-CoA for 3 min at 30 °C (according to refs *50*, *51*) with modifications introduced previously (*12*). GS activity was assayed as incorporation of [^{14}C]glucose from UDP-[^{14}C]glucose (4 μCi, 130 μM final concentration) into ethanol-precipitable glycogen by a postnuclear fraction from total defatted adipocyte homogenate (5500*g*/2 min supernatant) during incubation in the presence of 0.066/6.6 mM glucose-6-phosphate for 20 min at 30 °C as described (*12*) and calculated as fractional velocity according to ref *52*. Glucose transport in adipocytes was measured as uptake of 2-deoxy-[^{3}H]glucose (0.5 μCi, 100 μM final concentration) in the absence or presence of 20 μM cytochalasin B for 5 min at 25 °C using the oil centrifugation method as described (*49*, *53*). GLUT4 translocation was studied by determination of the amount of GLUT4 in plasma membranes isolated from the defatted homogenate of rat adipocytes by sucrose gradient centrifuation (according to refs *49*, *54*). After incubation of the adipocytes with insulin or PIG compound, the cells were treated with potassium cyanide (2 mM) to prevent GLUT4 redistribution. GLUT4 was identified by quantitative immunoprecipitation with anti-GLUT4 antibodies (raised in rabbits against the carboxy-terminal 16 amino acids of rat GLUT4) and subsequent separation of the immunopellets by SDS−PAGE and analysis by immunoblotting with the same antibodies and [^{125}I]protein A followed by phosphorimaging as described recently (*12*, *49*). The values were normalized by measuring protein concentration in each sample using the bicinchoninic acid assay (Pierce, Rockford, IL). Inhibition of lipolysis was assayed as the amount of glycerol in the defatted and perchloroacetic acid-treated homogenate (10000*g* supernatant, 15 min) from rat adipocytes which had been treated with isoproterenol (1 μM) and adenosine deaminase (1 U/mL) in KRP−Hepes containing 5.5 mM glucose for 120 min at 37 °C after prior incubation with PIG product or insulin for 20 min (see above) as detailed previously (*55*). Protein synthesis was determined as incorporation of [^{35}S]-methionine into trichloroacetic acid-precipitable protein in adipocytes which have been incubated in DMEM depleted of methionine in the presence of insulin/PIG compounds for 20 min at 37 °C (0.7×10^5 cells/mL) prior to addition of [^{35}S]methionine (6.5 μCi) and further incubation for 120 min as outlined recently (*48*). Glucose transport in diaphragms was measured by incubation of the washed hemidiaphragms in the presence of insulin/PIG compound with 20 mL of KRO buffer containing 1 mM 2-[^{3}H]deoxyglucose (2 μCi), 4 mM [U-^{14}C]sucrose (2 μCi), 2 mM pyruvate for 20 min at 30 °C under bubbling with 95% O_2/5% CO_2. Subsequent processing of the hemidiaphragms (blotting, removal of rib cage, solubilization, liquid scintillation counting) and calculation of the specific glucose transport rate as the difference between the total amount of deoxyglucose and sucrose associated with the diaphragm were performed as described previously (*15*). Glycogenesis was determined by incubation of the washed hemidiaphragms in the presence of insulin/PIG compound with 15 mL, each, of KRP−Hepes buffer containing 2 mM [U-^{14}C]glucose (5 μCi) for 20 min at 30 °C under continuous bubbling with 95% O_2/5% CO_2. Subsequent processing of the hemidiaphragms (removal of rib cage, washing, homogenization, centrifugation) and

determination of the amount of radiolabeled glycogen (precipitation, liquid scintillation counting) were performed as described previously (*12*).

Tyrosine Phosphorylation of IRS-1. After incubation with insulin/PIG compounds, the hemidiaphragms (80−100 mg wet weight) were rapidly liberated from the rib cage, rinsed once with homogenization buffer (25 mM Hepes/KOH, pH 7.4, 140 mM NaCl, 10% glycerol, 1 mM EDTA, 1 mM sodium vanadate, 50 mM sodium pyrophosphate, 100 mM NaF, 10 mM glycerol-3-phosphate, 0.2 mM PMSF, 10 μg/mL leupeptin, 10 μg/mL pepstatin, 5 μg/mL antipain, 25 μg/mL aprotinin), frozen in liquid N_2, and then homogenized in 2 mL of ice-cold homogenization buffer in a porcelain mortar on ice. After centrifugation (1500*g*, 10 min, 4 °C), the fat-free supernatant was supplemented with TX-100 (0.5% final concentration), incubated (30 min, 4 °C), and centrifuged (18000*g*, 20 min, 4 °C). One milliliter of the supernatant was precleared by addition of 50 μL of protein A/G-Sepharose (Pharmacia/LKB, Freiburg, Germany; 50 mg/mL of the same buffer) and centrifugation (see above). The supernatant was incubated with rabbit anti-rat carboxy-terminal IRS-1 antibodies (Upstate Biotechnology, Lake Placid; 1:500) for 2 h at 4 °C and then with protein A/G-Sepharose (5 mg) for 16 h at 4 °C. The precipitates were collected by centrifugation (12000*g*, 2 min) and washed three times with 1 mL, each, of homogenization buffer containing 1% TX-100, 250 mM NaCl and lacking glycerol and then twice with homogenization buffer lacking TX-100 and all salt ingredients. The immunoprecipitates were suspended in Laemmli sample buffer, heated (95 °C, 5 min), and centrifuged (12000*g*, 2 min). The supernatant was subjected to SDS−PAGE (8%) and immunoblotting with either mouse monoclonal anti-phosphotyrosine antibodies (Biomol, Hamburg, Germany; clone 3B12, 1:2000) or anti-IRS-1 antibodies (see above; 1:200) using decoration with [^{125}I]protein A (15 μCi/5 mL; Amersham-Buchler, Freiburg, Germany) and autoradiography according to published procedures (*56*). Quantitative evaluation was performed by phosphorimaging (Molecular Dynamics, Storm 840).

Calculation of Insulin-Mimetic Activity. Data from metabolic assays were calculated as stimulation factor above basal activity (absence of insulin/PIG compound) for lipogenesis, GPAT, glucose transport, and GLUT4 translocation or as difference between the basal and insulin/PIG compound-induced values for inhibition of lipolysis or vice versa for stimulation of GS and in each case normalized to the basal (set at 0%) and maximal insulin action (set at 100%; elicited at 10 nM insulin). At least four different adipocyte or six diaphragm preparations, respectively, with two to four independent incubations with insulin/PIG compounds for each preparation were performed. Each incubation was assayed at least in quadruplicate. Each point represents the medium value for the different cell preparations with ±SD indicated as bars. Concentration−response curves were fitted to the equation $y = a + b[x/(x + k)]$ using a Marquardt−Levenberg nonlinear least-squares algorithm. When plotted on linear-log axes, this equation gives a sigmoidal curve where the parameters are associated with the following properties: a = basal response; $a + b$ = maximal response; k = half-maximal concentration (EC_{50}); x = concentration of insulin.

RESULTS AND DISCUSSION

Chemical Synthesis of PIG Compounds of Varying Structural Complexity. A typical method for the synthesis of a PIG molecule is given in Scheme 1. The glycosidic linkages have been made stereoselective by the trichloroacetimidate methodology. For introduction of the phosphates, the tetrabenzylpyrophosphate/sodium hydride or the phosphitylation/oxidation protocol was preferred. The H-phosphonates were synthesized in reasonable yields with phosphoric acid/pivaloyl chloride. For introduction of the sulfates, a solution of trimethylamine−sulfur trioxide complex in pyridine was used. All compounds were characterized by mass, ^{1}H NMR, and ^{31}P NMR spectroscopy.

Structural Requirements for Insulin-Mimetic Activity of PIG Compounds on Glucose Metabolism and Transport. Forty-six PIG variants were synthesized consisting of the complete or shortened/mutated glycan moiety but lacking the peptide portion (Figure 1). They were tested for insulin-mimetic effects on key metabolic pathways and enzymes of lipogenesis (stimulation of lipogenesis at high glucose concentrations reflecting overall esterification and stimulation of GPAT activity representing the rate-limiting step of esterification), glycogenesis (stimulation of GS activity), and lipolysis in isolated rat adipocytes, which exhibit an exquisite sensitivity and responsiveness toward insulin. The PIG compounds were divided into four classes according to their insulin-mimetic activity with respect to stimulation of lipogenesis at high glucose concentration (Figure 1 and corresponding legend). Typical representatives of the four classes are compound **41**, HO-SO_2-O-6Manα1(Manα1-2)-2Manα1(6-HSO_3)-6Manα1-4GluNβ1-6(D)inositol-1,2-(cyclic)-phosphate; compound **37**, HO-PO(H)O-6Manα1(Manα1-2)-2Manα1-6Manα1-4GluNβ1-6(D)inositol-1,2-(cyclic)-phosphate; compound **7**, HO-PO(H)O-6Manα1-4GluN(1-6(L)inositol-1,2-(cyclic)-phosphate; and compound **1**, HO-PO(H)O-6Manα1-4GluNα1-6(L)inositol (Chart 1). Compounds **41** and **37** increased lipogenesis in a concentration-dependent manner up to 90% and 80% of MIR (at 20 μM), respectively, with EC_{50} values of 2.5 ± 0.9 and 4.9 ± 1.7 μM, respectively (Figure 2A). Compound **7** stimulated lipogenesis up to 20% of MIR (at 100 μM) only, whereas compound **1** was completely inactive. The same ranking of the four compounds (**41** > **37** ≫ **7** > **1**) was derived from the corresponding concentration−response curves for activation of GPAT (Figure 2B), GS (Figure 2C), and antilipolysis (Figure 2D) both with respect to MIR (GPAT: 90%, 90%, 25%, 0%; GS: 90%, 82%, 22%, 3%; inhibition of lipolysis: 95%, 95%, 42%, 0%) and the EC_{50} values (GPAT: 3.5 ± 0.8, 8.0 ± 1.1 μM, −, −; GS: 4.7 ± 1, 9.5 ± 1.5 μM, −, −; antilipolysis: 1.6 ± 0.5, 2.5 ± 0.5 μM, −, −). The maximal insulin-mimetic activity of compound **41**, as manifested in the assays for lipogenesis (at high glucose) as well as GPAT and GS activities, was comparable with that of the authentic PIG-P prepared from yeast Gce1p (*12*) with respect to the maximal response. However, the EC_{50} values of compound **41** were 5−10-fold higher than those of PIG-P. This, presumably, reflects the absence of the peptide moiety in the synthetic PIG compounds (W. Frick, A. Bauer, G. Müller, manuscript in preparation). Since under euglycemic as well as hyperglycemic conditions glucose transport is regarded as rate-limiting for lipid and glycogen synthesis

in fat and muscle tissues (*57*), we studied whether the PIG compounds exert insulin-mimetic activity on glucose transport in isolated rat adipocytes. Compound **41** was the most potent compound in stimulating glucose transport [measured as uptake of 2-deoxyglucose (Figure 3A) or as lipogenesis at low glucose concentration (Figure 3B)] approaching 45−50% of MIR (at 50 μM) with EC_{20} values of 4−6 μM in comparison to compound **37** (35−40% of MIR; EC_{20} values of 10−20 μM), compound **45** (25−30% of MIR; EC_{20} values of 15−30 μM), compound **7** (10−15% of MIR), and compound **1** (almost inactive).

Glucose transport stimulation by insulin in insulin-sensitive muscle and fat cells is based on increased translocation of GLUT4 from internal stores to the plasma membranes (for a review, see ref *58*). Compounds **41**, **37**, **45**, and **7** increased the amount of GLUT4 at the cell surface in a concentration-dependent fashion up to 50% of MIR as revealed by immunoprecipitation and subsequent immunoblotting of GLUT4 from plasma membranes of adipocytes treated with the compounds (Figure 4). GLUT4 translocation was not induced by compound **1**. The maximal responses and EC_{50} values of these compounds closely match those for glucose transport activation, the relative ranking of the compounds with regard to both parameters (**41** > **37** ≥ **45** ≫ **7** > **1**) is identical for stimulation of glucose transport and GLUT4 translocation (Figure 3C).

Numerous studies have described a discrepancy between glucose transport activation and GLUT4 translocation provoked by insulin in isolated rat adipocytes (*59*, *60*). This has been interpreted as the presence of glucose transporter molecules that are catalytically inactive or partially occluded from the plasma membrane (*61*). The PIG-induced glucose transport activation, however, can be fully explained with GLUT4 translocation (see Figures 3 and 4). This suggests

A

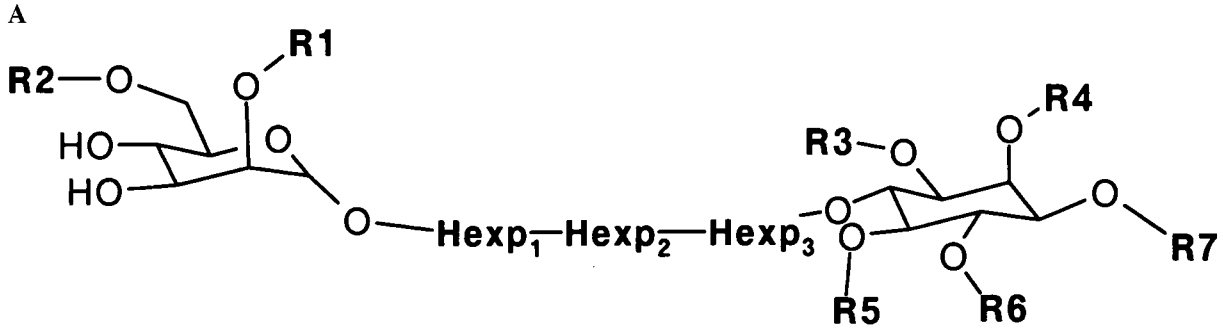

No	Structure	R1	R2	$Hexp_1$	$Hexp_2$	$Hexp_3$	R3 R4	R5 R6	R7	Activity
1	HO-PO(H)O-6Manα1-4GluNα1-6(L)inositol	H	H-P			4GluNα	H H	H H	H	A
2	HO-PO(H)O-6Manα1-6Manα1-6Manα1-6Manα1-6Manα1-6(L)inositol-3-phosphate	H	6H-P Manα	6Manα	6Manα	6Manα	H H	H H	P	A
3	6Manα1-6Manα1-6Manα1-6Manα1-6Manα1-6(L)inositol-3-phosphate	H	Manα	6Manα	6Manα	6Manα	H H	H H	P	A
4	HO-PO(H)O-6Manα1-6Manα1-6Manα1-6Manα1-3GluNβ1-6(L)inositol-3-phosphate	H	6H-P Manα	6Manα	6Manα	3GluNβ	H H	H H	P	A
5	HO-PO(H)O-6Manα1(Manα1−2)-2Manα1(6-PO(H)OH)-6Manα1-6Manα-1-6(D,L)inositol-1,2-4,5(cyclic)-diphosphate	Manα	H-P	6H-P 2Manα	6Manα	6Manα	cyclic P	cyclic P	H	B
6	HO-PO(OH)O-6Manα1(Manα1−2)-2Manα1(6-$PO(OH)_2$)-6Manα1-6Manα-1-6(D,L)inositol-1,2-4,5(cyclic)-diphosphate	Manα	P	6-P 2Manα	6Manα	6Manα	cyclic P	cyclic P	H	B
7	Manα1-4GluNα1-6(L)inositol-1,2-(cyclic)-phosphate	H	H			4GluNα	cyclic P	H H	H	B
8	HO-PO(H)O-6Manα1-4GluNα1-6(L)inositol-1,2-(cyclic)-phosphate	H	H-P			4GluNα	cyclic P	H H	H	B
9	HO-SO_2-O-6Manα1(Manα1−2)-2Manα1(6-HSO_3)-6Manα1-6Manα-1-6(D,L)inositol-1,2-4,5(cyclic)-diphosphate	Manα	S	6-S 2Manα	6Manα	6Manα	cyclic P	cyclic P	H	B
10	HO-PO(H)O-6Manα1(Manα1−2)-2Manα1-6Manα1-3GluNβ1-6(L)-inositol-3-phosphate	Manα	H-P	2Manα	6Manα	3GluNβ	H H	H H	P	B
11	Manα1(Manα1−2)-2Manα1-6Manα1-3GluNβ1-6(L)inositol-3-phosphate	Manα	H	2Manα	6Manα	3GluNβ	H H	H H	P	B
12	HO-PO(H)O-6Manα1(Manα1−2)-6Manα1-6Manα1-6Manα1-6Manα1-6(L)inositol-3-phosphate	H	Manα1−2Manα (6H-P)	6Manα	6Manα	6Manα	H H	H H	P	B
13	HO-PO(H)O-6Manα1-2Manα1(6-PO(H)OH)-6Manα1-3GluNβ1-6(L)inositol-3-phosphate	H	H-P	6H-P 2Manα	6Manα	3GluNβ	H H	H H	P	C
14	H_2N-CO-O-6Manα1(Manα1−2)-2Manα1(6-$CONH_2$)-6Manα1-3GluNβ1-6(L)inositol-3-phosphate	Manα	Carb	6Carb 2Manα	6Manα	3GluNβ	H H	H H	P	C
15	Manα1-2Manα1-2Manα1(6-HSO_3)-6Manα1-6Manα1-6(D,L)inositol-3-phosphate	Manα	H	6-S 2Manα	6Manα	6Manα	H H	H H	P	C
16	HO-PO(H)O-6Manα1(Manα1−2)-2Manα1(6-PO(H)OH)-6Manα1-3GluNβ1-6(L)inositol-3-phosphate	Manα	H-P	6H-P 2Manα	6Manα	3GluNβ	H H	H H	P	C
17	Manα1-2Manα1-2Manα1(6-PO(H)OH)-6Manα1-3GluNβ1-6(L)inositol-3-phosphate	Manα	H	6H-P 2Manα	6Manα	3GluNβ	H H	H H	P	D
18	Manα1(Manα1−2)-2Manα1(6-HSO_3)-6Manα1-3GluNβ1-6(L)inositol-3-phosphate	Manα	H	6-S 2Manα	6Manα	3GluNβ	H H	H H	P	D
19	HO-SO_2-O-6Manα1(Manα1−2)-2Manα1(6-HSO_3)-6Manα1-3GluNβ1-6(L)inositol-3-phosphate	Manα	S	6-S 2Manα	6Manα	3GluNβ	H H	H H	P	D

B

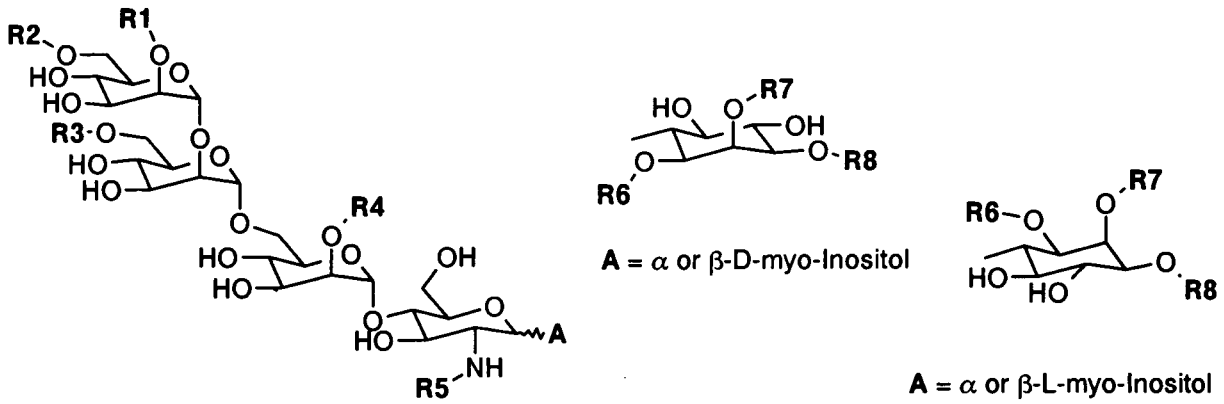

No	Structure	R1	R2	R3	R4	R5	R6 R7	R8	A	Activity
20	Manα1-2Manα1- 6Manα1-4GluNα1-6(L)-inositol-1,2-(cyclic)-phosphate	H	H	H	H	H	cyclic P	H	α-L	A
21	Manα1-2Manα1-2Manα1- 6Manα1-4GluNα1-6(L)-inositol-1-phosphate	Manα	H	H	H	H	H H	H	α-L	B
22	Manα1-2Manα1-2Manα1(6-HSO_3)-6Manα1-4GluNβ1-6(D)-inositol-1,2-(cyclic)-phosphat-3-phosphate	Manα	H	S	H	H	cyclic P	P	β-D	B
23	NH_2-$(CH_2)_2$-O-PO(OH)O-6Manα1-2Manα1- 6Manα1-4GluNβ1-6(L)-inositol-1-phosphate	H	EtNP	H	H	H	P H	H	β-L	B
24	Manα1-2Manα1–2Manα1-2Manα1-6Manα1-4GluNβ1-6(D,L)-inositol	Manα1-2Manα	H	H	H	H	H H	H	β–D,L	B
25	Manα1-2Manα1-2Manα1- 6Manα1-4GluNβ1-6(L)-inositol-1,2-(cyclic)-phosphate	Manα	H	H	H	H	cyclic P	H	β-L	B
26	Manα1–2Manα1-2Manα1-6Manα1-4GluNAcβ1-6(D)-inositol-1,2-(cyclic)-phosphate	Manα	H	H	H	Ac	cyclic P	H	β-D	B
27	Manα1–2Manα1-2Manα1-6Manα1-4GluNβ1-6(D)-inositol-1,2-(cyclic)-phosphate	Manα	H	H	H	H	cyclic P	H	β-D	B
28	Manα1-2Manα1–2Manα1-2Manα1-6Manα1-4GluNβ1-6(D)inositol-1,2-(cyclic)-phosphate	Manα1-2Manα	H	H	H	H	cyclic P	H	β-D	B
29	NH_2-$(CH_2)_2$-O-PO(OH)O-6Manα1-2Manα1- 6Manα1-4GluNα1-6(L)-inositol-1,2-(cyclic)-phosphate	H	EtNP	H	H	H	cyclic P	H	α-L	C
30	HO-PO(H)O-6Manα1(Manα1–2)-2Manα1(6EtNP)-6Manα1(2EtNP)-4GluNβ1-6(D)-inositol-1,2-(cyclic)-phosphate	Manα	H-P	EtNP	EtNP	H	cyclic P	H	β-D	C
31	HO-PO(H)O-6Manα1(Manα1–2)-2Manα1- 6Manα1-4GluNα1-6(L)-inositol-1-or-2-phosphate	Manα	H-P	H	H	H	P, H	H	α-L	C
32	Manα1(Manα1–2)-2Manα1- 6Manα1-4GluNα1-6(D)-inositol-1-or-2-phosphate	Manα	H	H	H	H	P, H	H	α-D	C
33	HO-PO(H)O-6Manα1(Manα1–2)-2Manα1- 6Manα1-4GluNβ1-6(L)-inositol-1,2-(cyclic)-phosphate	Manα	H-P	H	H	H	cyclic P	H	β-L	C
34	HO-PO(H)O-6Manα1(Manα1–2)-2Manα1- 6Manα1-4GluN(HSO_3)β1-6(L)-inositol-1,2-(cyclic)-phosphate	Manα	H-P	H	H	S	cyclic P	H	β-L	C
35	HO-PO(H)O-6Manα1(Manα1–2)-2Manα1-6Manα1-4GluNβ1-6(D)-inositol-1,2-(cyclic)-thiophosphate	Manα	H-P	H	H	H	cyclic PS	H	β-D	C
36	H_2N-CO-6Manα1(Manα1–2)-2Manα1- 6Manα1-4GluNβ1-6(D)-inositol-1,2-(cyclic)-phosphate	Manα	Carb	H	H	H	cyclic P	H	β-D	C
37	HO-PO(H)O-6Manα1(Manα1–2)-2Manα1- 6Manα1-4GluNβ1-6(D)-inositol-1,2-(cyclic)-phosphate	Manα	H-P	H	H	H	cyclic P	H	β-D	C
38	HO-PO(OH)O-6Manα1(Manα1–2)-2Manα1(6-PO(OH)$_2$)-6Manα1 -4GluNβ1-6(D)-inositol-1,2-(cyclic)-phosphate	Manα	P	P	H	H	cyclic P	H	β-D	D
39	HO-SO_2-6Manα1(Manα1–2)-2Manα1- 6Manα1-4GluNβ1-6(D)-inositol-1,2-(cyclic)-phosphate	Manα	S	H	H	H	cyclic P	H	β-D	D
40	HO-PO(H)O-6Manα1(Manα1–2)-2Manα1(6-PO(H)OH)-6Manα1 -4GluNβ1-6(D)-inositol-1,2-(cyclic)-phosphate	Manα	H-P	H-P	H	H	cyclic P	H	β-D	D
41	HO-SO_2-O-6Manα1(Manα1–2)-2Manα1(6-HSO_3)-6Manα1 -4GluNβ1-6(D)-inositol-1,2-(cyclic)-phosphate	Manα	S	S	H	H	cyclic P	H	β-D	D

C

No	Structure	Activity
42	GalNβ1-4-(L)-pinitol	A
43	GluNα1-6(D)inositol-1,2-(cyclic)-phosphate	A
44	Manα1-4GluNα1-O-1(2,3-cyclic-phosphatyl)n-propyl	A
45	Manα1-2Manα1-2Manα1(6-HSO_3)-6Manα1-3GluNβ1-3(D oder L)inositol-6-sulfat	C
46	Manα1-2Manα1-2Manα1(6-HSO_3)-6Manα1-3GluNβ1-3(D oder L)inositol-6-phosphat	C

FIGURE 1: Structure and insulin-mimetic activity of various PIG compounds. Isolated rat adipocytes were incubated with increasing concentrations (0.1−200 μM) of compounds **1**−**46** and then assayed for lipogenesis and glucose transport as described in Materials and Methods. MIR and $EC_{20/50}$ values were derived from the corresponding concentration−response curves. The compounds are arranged according to increasing maximal activity (lipogenesis) and divided into four classes according to the following criteria: class A, MIR < 20%; class B, MIR 20−49%, EC_{20} 25−200 μM; class C, MIR 50−80%, EC_{50} 10−100 μM; class D, MIR > 80%, EC_{50} 3−30 μM.

Chart 1: Structures of **41**, **37**, **7**, and **1**, Typical Representatives of the Four Classes of PIG Compounds with Varying Insulin-Mimetic Activity

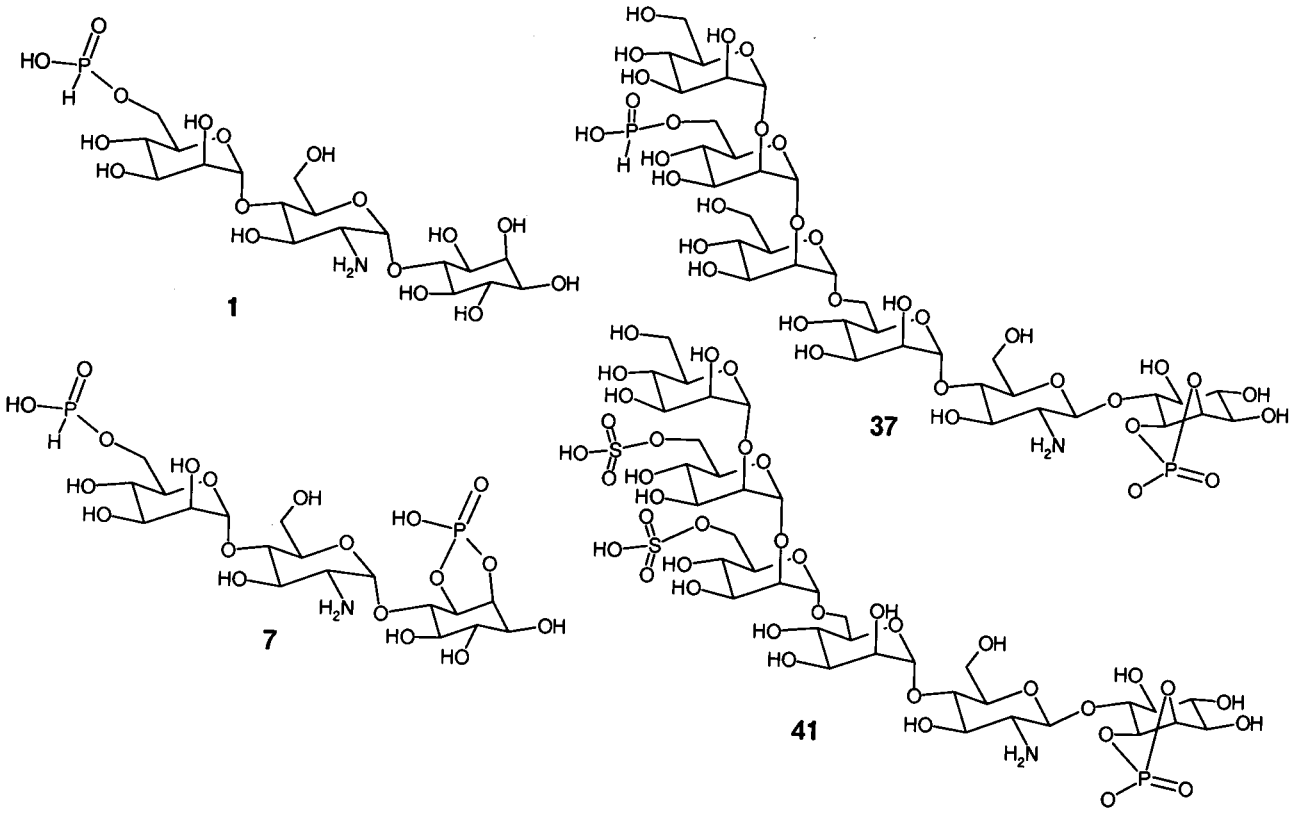

that PIG compounds efficiently trigger (i) movement of GLUT4 vesicles to the plasma membrane, (ii) their fusion with the plasma membrane and thereby proper cell surface exposure of GLUT4 molecules, and, finally, (iii) activation of the GLUT4 intrinsic transport function. The observed about half-maximal insulin activation of glucose transport and GLUT4 translocation but almost full insulin activation of the key enzymes of lipid and glycogen synthesis, GPAT and GS, respectively, suggests that regulation of these enzymes is the primary and predominant effect of potent PIG molecules, like compounds **41** and **37**, on glucose and lipid metabolism in adipocytes.

The 46 PIG compounds have been divided into four classes, A, B, C, D, according to their insulin-mimetic activity in isolated rat adipocytes (Figure 1). The analysis of the relationship between structure and activity suggests that the complete authentic core glycan consisting of the backbone of three mannose residues, the glucosamine, and inositol moieties including the mannose side branch in correct glycosidic linkage is required for potent insulin-mimetic activity (classes C and D). In contrast, both termini of the core glycan with regard to the presence and position of phosphate/sulfate moieties as well as the type of linkage determine in a very distinct and barely predictable fashion the insulin-mimetic activity ranging from no negative impact at all (e.g., class C → C) to significant decreases (e.g., class D → C) or increases (e.g., class B → C) in activity. This was exemplified in a considerable loss in insulin-mimetic activity upon exchange of the terminal sulfate moiety for H-phosphate, phosphate, or carbamide, in that order (**41** > **40** > **38** or **39** > **37** > **36**), and in the surprising finding that a β-glycosidic linkage between inositol and glucosamine affected the insulin-mimetic activity in a positive fashion compared to the corresponding naturally occurring α-glycosidic bond (Figure 1B). In contrast, the presence of D- or L-inositol within a given PIG structure had a minor impact on its insulin-mimetic activity only. In agreement with the necessity of a certain structural complexity for induction of pronounced insulin-mimetic activity (i.e., classes C and D) is our finding that the activities of the simple compounds **42** and **43** (Figure 1C), consisting of (phospho)disaccharides only and synthesized previously also by other laboratories (*38*, *43*), were very low (class A) compared to that of PIG molecules harboring the complete core glycan. Despite these obvious limitations in structural simplification of PIG compounds retaining almost full insulin-mimetic activity, we succeeded in considerably reducing the structural complexity and thereby the synthesis expenditure for compounds with quite pronounced activity. This is exemplified best by compounds **37** vs **15**, the synthesis of which required 52 and 33 steps, respectively. Nevertheless, both molecules exhibited almost the same insulin-mimetic activity in the range of class C compounds.

Potent PIG Compounds Exhibit Insulin-Mimetic Activity in Adipocytes and Diaphragms with Reduced Responsiveness toward Insulin. Next we studied whether the synthetic PIG compounds are functional in two in vitro models for cells desensitized toward insulin. For this, the adipocytes were subjected to limited digestion with trypsin (Figure 5A,B) or made insulin-resistant by primary culture with high concentrations of glucose and insulin (Figure 5C,D) and then assayed for glucose transport activation by increasing concentrations of insulin and compound **37** (open circles) in parallel with control adipocytes which had been mock-

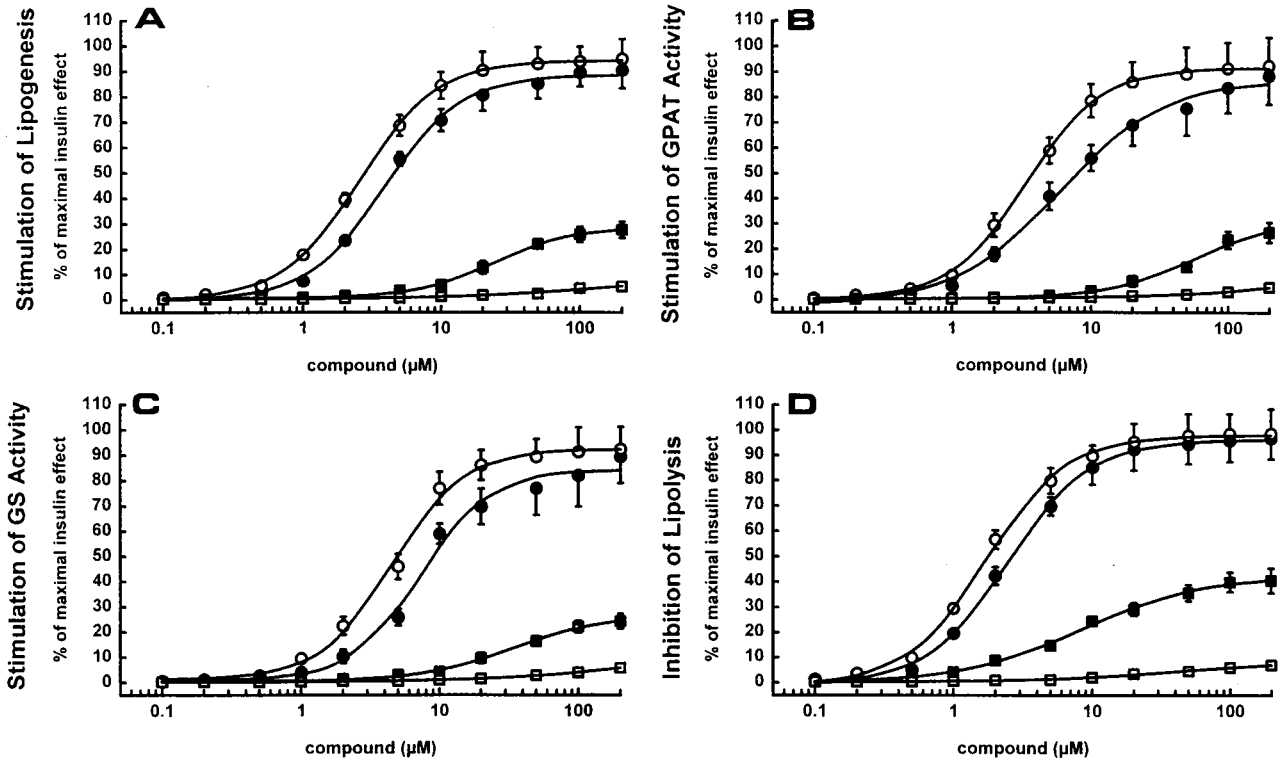

FIGURE 2: Effects of compounds **41**, **37**, **7**, and **1** on key metabolic pathways and enzymes in adipocytes. Isolated rat adipocytes were incubated with increasing concentrations of compounds **41** (open circles), **37** (closed circles), **7** (closed squares), and **1** (open squares) or 10 nM human insulin and then assayed for stimulation of lipogenesis at high glucose (A), GPAT (B), and GS (C) and inhibition of lipolysis (D). The insulin-mimetic activity was calculated as percent of the maximal stimulation factor provoked by insulin (A, B), of the maximal insulin stimulation of GS (C, difference of fractional velocity between presence and absence of insulin/PIG compound), and of the maximal insulin inhibition of isoproterenol-stimulated lipolysis (D, difference of glycerol release between the absence and presence of insulin/PIG compound). Maximal insulin stimulation of lipogenesis was 5.9-fold corresponding to 3.7 nmol of glucose incorporated into lipids per 3.5×10^5 cells and 90 min, of GPAT was 2.7-fold corresponding to 0.8 nmol of glycerol-3-phosphate incorporated into lipids per 100 μg of microsomal protein and 3 min, and of GS was 4.5-fold corresponding to an increase of the fractional velocity from 0.06 to 0.27 [a fractional velocity of 1 (presence of glucose-6-phosphate) corresponds to 23 nmol of glucose incorporated into glycogen per mg of homogenate protein and min]. Maximal insulin inhibition of lipolysis corresponds to 2145 nmol of glycerol released per 3.5×10^5 cells and 1 h (difference between isoproterenol-induced cells in the absence and presence of insulin).

treated under the same incubation conditions (closed circles). Both treatments led to drastic reductions of MIR and insulin sensitivity (i.e., rightward shift of the concentration−response curves; Figure 5A,C, open circles) with the trypsin-treated cells being almost completely unresponsive toward insulin. In contrast, both the trypsin-treated and cultured adipocytes maintained almost full sensitivity and responsiveness toward compound **37** (Figure 5B,D, open circles) compared to control cells (closed circles), which accounted for about 40% of MIR measured in control cells. Glucose transport activation by compound **41** was also not impaired in trypsin-treated or cultured adipocytes compared to control cells (data not shown). Thus, the synthetic PIG compounds seem to bypass the insulin receptor kinase and the putative insulin signaling defect in insulin-resistant cultured adipocytes.

Consequently, we studied whether the PIG compounds manage to induce GLUT4 translocation in adipocytes derived from a typical animal model of non-insulin-dependent diabetes mellitus, the Zucker fatty rat, which is characterized by pronounced insulin resistance of their muscle and adipose tissue (*62*, *63*; for a review, see ref *64*). Insulin increased the amount of GLUT4 recovered with the plasma membranes by 3.6 ± 0.6-fold at maximum (Figure 6, lane 9) with a concentration−response curve considerably shifted to the right (lanes 7−9) in comparison to that of adipocytes from normal Wistar rats (see Figure 3C). This impaired insulin responsiveness and sensitivity reflect the insulin-resistant state of adipocytes from Zucker fatty rats. In contrast, GLUT4 translocation was stimulated by compounds **41** (Figure 6, lanes 2−6) and **37** (lanes 14−16) in a concentration-dependent manner to up to 5.9 ± 0.9-fold and 2.1 ± 0.3-fold, respectively, with no apparent loss of sensitivity toward these agents compared to adipocytes from normal rats. Compound **7** showed a very moderate effect (1.4 ± 0.2-fold) on GLUT4 translocation only (lanes 11−13). Thus PIG compounds exert insulin-mimetic activity in adipocytes from insulin-resistant rats with maximal responses comparable to and a relative ranking of their potency identical for cells from insulin-sensitive animals. Remarkably, compound **41** was more potent in provoking GLUT4 translocation in adipocytes from Zucker fatty rats than insulin (see Figure 6, compare lanes 4−6 with 7−9).

Many compounds (e.g., lipids, denatured proteins, ions) activate glucose metabolism in rat adipocytes in vitro, but they do so at high concentrations (at least millimolar range) with rather low efficiency (10−30% of MIR). Moreover, in most cases, these irrelevant compounds are used as complex and crude mixtures (e.g., complete lipid or protein extracts from cells). So far there is no report on a defined ion, lipid, protein, or sugar solution that exerts almost full insulin-mimetic activity at concentrations of 10 μM. Incubation of isolated rat adipocytes with chemically defined

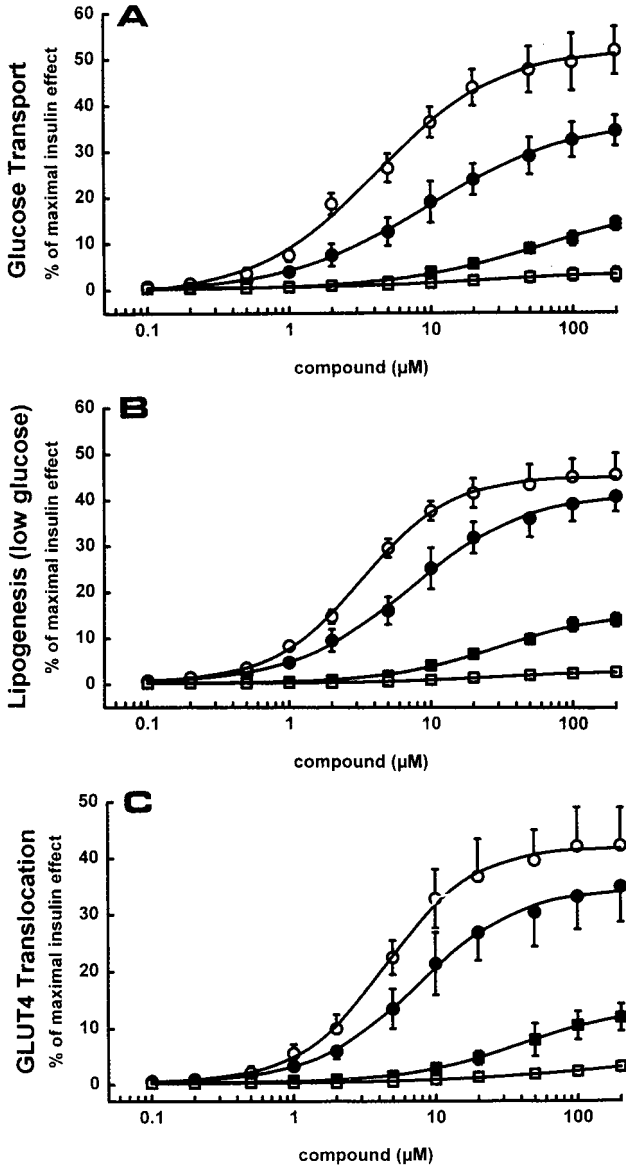

FIGURE 3: Effects of compounds **41**, **37**, **7**, and **1** on glucose transport in adipocytes. Isolated rat adipocytes were incubated with increasing concentrations of compounds **41** (open circles), **37** (closed circles), **7** (closed squares), and **1** (open squares) or 10 nM human insulin and then assayed for glucose transport (A), lipogenesis at low glucose (B), and GLUT4 translocation (C). The insulin-mimetic activity was calculated as percent of the maximal stimulation factor provoked by insulin. Maximal insulin stimulation of glucose transport was 17.6-fold corresponding to 0.35 nmol of deoxyglucose transported per 3×10^4 cells and 5 min, of lipogenesis was 24.9-fold corresponding 22.3 nmol of glucose incorporated into lipids per 0.5×10^5 cells and 90 min, and for GLUT4 translocation was 6.9-fold (the amount of GLUT4 in the plasma membrane of basal cells was set at 1).

molecules at concentrations in the micromolar range has to be regarded as a reliable and specific system. To further substantiate the specificity of the insulin-mimetic activity of the PIG compounds, we used a different model system for assaying insulin action, the isolated rat diaphragm, which may be regarded as less sensitive toward irrelevant compounds. Furthermore skeletal muscle tissue is the predominant site for nonoxidative insulin-dependent glucose disposal. We studied the effects of the PIG compounds on glucose metabolism (as manifested in glucose transport and glycogenesis) in isolated diaphragms from normal Wistar rats and

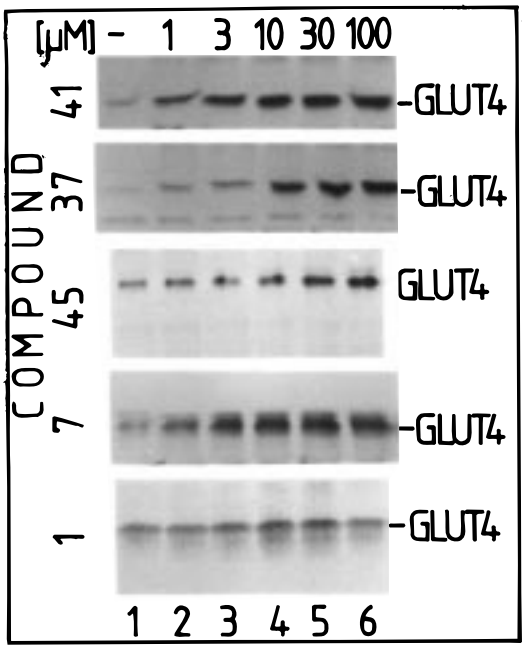

FIGURE 4: Effects of compounds **41**, **37**, **7**, and **1** on GLUT4 translocation in adipocytes from normal rats. Isolated rat adipocytes from Wistar rats were incubated in the absence (lane 1) or presence of increasing concentrations of compounds **41**, **37**, **45**, **7**, or **1** (lanes 2−6) for 20 min at 37 °C. Plasma membranes were isolated from the total defatted homogenate, and identical amounts of protein were assayed for GLUT4 content by successive quantitative immunoprecipitation (using anti-GLUT4 antibody and protein A-Sepharose) and immunoblotting (using anti-GLUT4 antibody and [^{125}I]protein A). An autoradiogram from a typical experiment is shown thrice repeated with similar results.

insulin-resistant Zucker fatty rats. Compounds **41** and **37** increased 2-deoxyglucose transport in normal diaphragms to up to 90−95% (at 20 μM) of MIR (at 300 nM) with EC_{50} values of 3.5 ± 0.6 and 8.3 ± 1.5 μM, respectively (Table 1). Compound **7** was less efficient with 40% (at 20 μM) of MIR. Compound **1** was completely ineffective (data not shown). In diaphragms from Zucker fatty rats, the insulin stimulation of glucose transport was rather modest (1.5-fold above basal) compared to 4-fold in diaphragms from Wistar rats. This was based on both significantly increased basal and drastically diminished insulin-induced transport. Thus diaphragms from Zucker fatty rats display a pronounced insulin resistance of glucose transport. Remarkably, in contrast to the magnitude of insulin resistance, the loss of responsiveness of glucose transport toward compounds **41**, **37**, and **7** in diaphragms from Zucker fatty rats vs normal rats was moderate (2.4 ± 0.5-fold vs 3.8 ± 0.8-fold and 2.1 ± 0.4-fold vs 3.7 ± 0.5-fold). In consequence, the incremental stimulation of glucose transport by compounds **41**, **37**, and **7** exceeded that of insulin by up to 260%, 210%, and 120%, respectively.

The data on the activation of glycogen synthesis in normal and insulin-resistant diaphragms led to similar conclusions. Compounds **41**, **37**, and **7** increased glycogenesis in normal diaphragms to up to 70%, 65%, and 33% (at 20 μM), respectively, of MIR (at 300 nM) with EC_{50} values of 3.3 ± 0.5 μM (compound **41**) and 7.1 ± 2.0 μM (compound **37**) (Table 2). Again, compound **1** was inactive (data not shown). As expected, the diaphragms from Zucker fatty rats exhibited significant insulin resistance as manifasted in

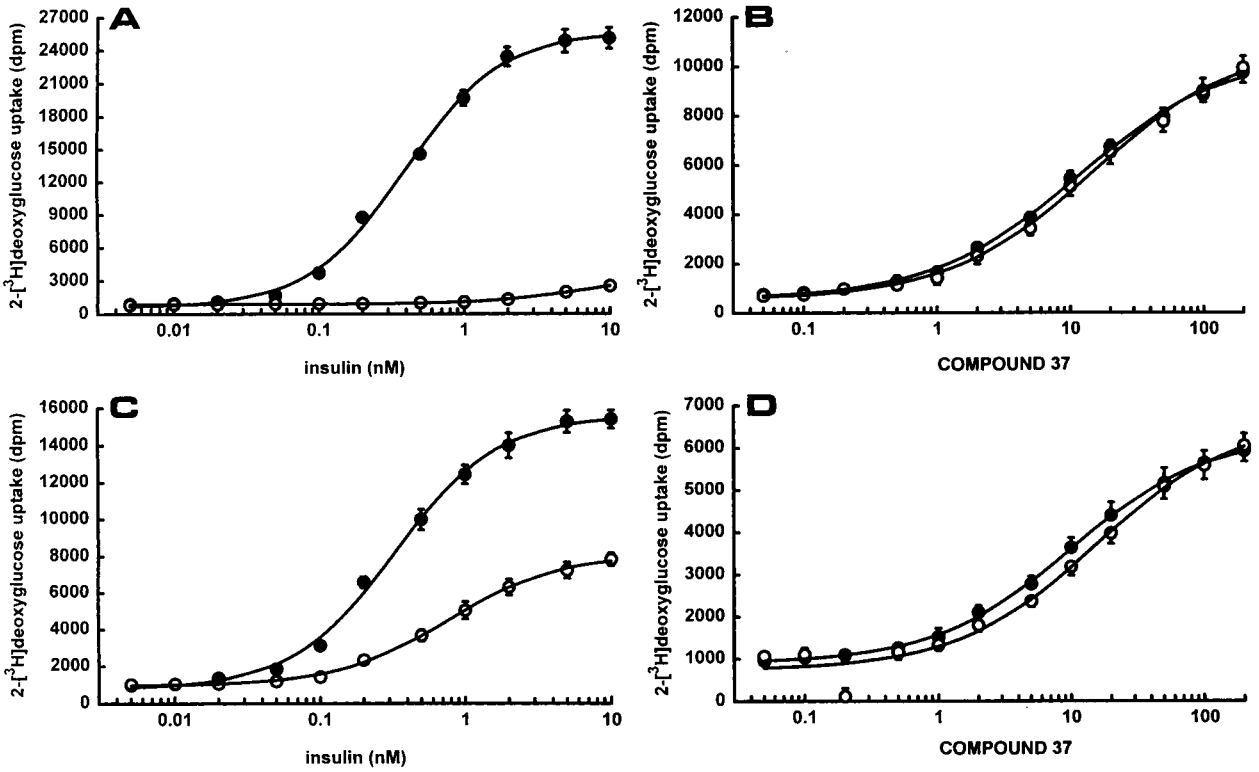

FIGURE 5: Effect of desensitization of adipocytes toward insulin action on the insulin-mimetic activity of compound **37**. Control (A, B; closed circles) and trypsinized adipocytes (A, B; open circles), control adipocytes (C, D; closed circles), and adipocytes cultured in the presence of glucose and insulin (C, D; open circles) were incubated with increasing concentrations of insulin (A, C) or compound **37** (B, D) and then assayed for glucose transport; 1000 dpm correspond to 93 pmol of 2-deoxyglucose transported per 3×10^4 cells and 5 min.

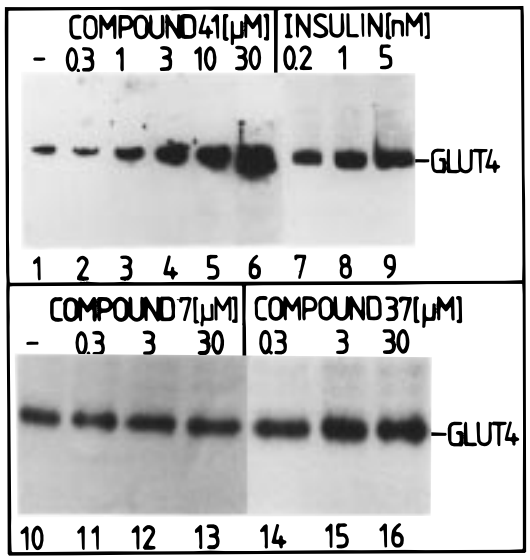

FIGURE 6: Effects of compounds **41**, **37**, and **7** on GLUT4 translocation in adipocytes from insulin-resistant rats. Isolated rat adipocytes from Zucker fatty rats were incubated in the absence (lanes 1, 10) or presence of increasing concentrations of compounds **41** (lanes 2−6), **37** (lanes 14−16), and **7** (lanes 11−13) or human insulin (lanes 7−9) for 20 min at 37 °C. Plasma membranes were isolated from the total defatted homogenate, and identical amounts of protein were assayed for GLUT4 content by successive quantitative immunoprecipitation and immunoblotting as described in Materials and Methods. An autoradiogram from a typical experiment is shown repeated twice with similar results.

elevated basal and reduced insulin-stimulated glycogenesis resulting in a 1.9 ± 0.3-fold MIR compared to 4.1 ± 0.7-fold MIR in normal diaphragms. Compounds **41** and **37** exceeded the insulin action on glycogenesis in insulin-resistant diaphragms with 2.4 ± 0.3-fold and 2.2 ± 0.3-fold increases, respectively. In conclusion, PIG compounds apparently manage to activate glucose transport and glycogenesis in diaphragms from insulin-resistant and normal rats with almost the same potency and with the identical relative ranking between them. These observations with cells from insulin-resistant animals nicely complement the presented data obtained with cells desensitized for insulin action in vitro (see above) and our previous observations with PIG-P

Table 1: Effects of Compounds **41**, **37**, and **7** on Glucose Transport in Isolated Diaphragms from Normal and Insulin-Resistant Rats[a]

	glucose transport in diaphragms (pmol/mg/min)				
	normal	insulin-resistant		normal	insulin-resistant
basal	175 ± 24	249 ± 59			
	Insulin (nM)			Compound **41** (μM)	
1	239 ± 30	266 ± 44	0.5	198 ± 22	239 ± 30
3	330 ± 52	285 ± 37	1	255 ± 31	308 ± 39
10	448 ± 45	322 ± 32	2	374 ± 48	397 ± 42
30	582 ± 70	353 ± 49	5	559 ± 60	496 ± 51
100	651 ± 63	370 ± 39	10	619 ± 52	552 ± 71
300	697 ± 105	381 ± 77	20	670 ± 49	599 ± 63
	Compound **37** (μM)			Compound **7** (μM)	
0.5	205 ± 33	263 ± 26	0.5	177 ± 23	235 ± 39
1	226 ± 27	282 ± 30	1	186 ± 20	242 ± 33
2	267 ± 29	339 ± 27	2	244 ± 31	269 ± 30
5	383 ± 40	390 ± 38	5	307 ± 38	336 ± 44
10	530 ± 45	481 ± 44	10	369 ± 29	368 ± 39
20	654 ± 38	533 ± 50	20	396 ± 34	402 ± 35

[a] Isolated rat diaphragms from normal Wistar or insulin-resistant Zucker fatty rats were incubated in the absence or presence of increasing concentrations of human insulin or compounds **41**, **37**, and **7** and then assayed for glucose transport as described in Materials and Methods.

Table 2: Effects of Compounds **41**, **37**, **7**, and **1** on Glycogenesis in Isolated Diaphragms from Normal and Insulin-Resistant Rats[a]

	glycogenesis in diaphragms (dpm/mg of wet weight/20 min)				
	normal	insulin-resistant		normal	insulin-resistant
basal	2134 ± 397	3045 ± 505			
	Insulin (nM)			Compound **41** (μM)	
1	2487 ± 488	2896 ± 471	0.5	2684 ± 578	3314 ± 507
3	3074 ± 522	3183 ± 555	1	3302 ± 522	3974 ± 634
10	4266 ± 604	3471 ± 504	2	4511 ± 680	5038 ± 813
30	6580 ± 577	4121 ± 688	5	5673 ± 802	6107 ± 888
100	8124 ± 979	5285 ± 845	10	6407 ± 915	6891 ± 904
300	8650 ± 1105	5760 ± 803	20	6855 ± 893	7186 ± 995
	Compound **37** (μM)			Compound **7** (μM)	
0.5	2355 ± 401	3199 ± 506	0.5	2206 ± 510	3196 ± 588
1	2564 ± 499	3406 ± 611	1	2488 ± 467	3055 ± 523
2	3122 ± 610	3893 ± 570	2	2972 ± 602	3587 ± 634
5	4231 ± 557	4850 ± 713	5	3585 ± 762	4359 ± 714
10	5508 ± 734	5996 ± 844	10	4031 ± 665	4784 ± 770
20	6350 ± 814	6511 ± 789	20	4260 ± 709	4949 ± 748

[a] Isolated rat diaphragms from normal Wistar or insulin-resistant Zucker fatty rats were incubated in the absence or presence of increasing concentrations of human insulin or compounds **41**, **37**, and **7** and then assayed for glycogenesis as described in Materials and Methods.

from yeast using the same cellular models for insulin resistance (*12*). Taken together, these data suggest that in rat adipocytes and diaphragms the PIG compounds share a common site of interference within the insulin signaling cascade, which is located downstream of the putative insulin resistance block but upstream of the branching point between the signaling pathways to the glucose transport system and GS.

PIG Compounds and Insulin Have Some Signaling Steps in Common. In a previous study for elucidation of the molecular basis of the insulin-mimetic activity of PIG-P from yeast, we analyzed its effect on the early steps of insulin signaling in isolated rat cardiomyocytes and adipocytes (*15*). It was found that PIG-P does not stimulate the insulin receptor tyrosine kinase but induces significant tyrosine phosphorylation of IRS-1 and activation of phosphatidylinositol 3-kinase which is prerequisite for glucose transport activation by the compound. Thus, insulin and PIG-P signaling seems to be divergent upstream of IRS-1 but may converge at that level. As a first indication for the existence of common steps in signaling by the PIG compounds and insulin, we studied whether there is interference of the insulin-mimetic activity of the PIG compounds with insulin action and vice versa. For this, rat adipocytes were pretreated with various concentrations of compounds **37** and **41** or insulin and then tested for sensitivity toward insulin or compounds **37** and **41**, respectively, by incubation with increasing concentrations of agent and subsequent assay for lipogenesis (in the presence of high glucose). Low concentrations of PIG compound (Figure 7A, 1 μM **37**; B, 0.5 μM **41**), which per se led to an intrinsic insulin-mimetic activity of 5−10% of MIR only, increased significantly both the maximal response (from 100% to about 140% of MIR) and the insulin sensitivity (EC_{50} value from 0.3 to 0.07 μM) of the cells (Figure 7A,B). Thus, compounds **37** and **41** in the low micromolar range increased the sensitivity of rat adipocytes toward insulin action. At higher concentrations (2−20 μM), the insulin-mimetic activity of the compounds was additive to the insulin action to up to 0.1 nM insulin concentration (i.e., to up to about 130% of MIR) and subadditive at insulin concentrations above. A similar phenomenon was observed with the reciprocal experimental design, i.e., when the effect of insulin on the sensitivity of adipocytes toward the synthetic PIG compounds was measured (Figure 7C,D). Insulin at a concentration of 0.05 nM, which elicited 15−20% of MIR, significantly enhanced the maximal **37**- and **41**-induced effects (Figure 7C,D) from 85% to 140% of MIR accompanied by a reduction of the EC_{50} values from 3 to 0.07 μM. Thus, insulin at subnanomolar concentrations increased the sensitivity of rat adipocytes toward PIG action. At 0.2 nM, the insulin effect was roughly additive to the PIG action over the total PIG concentration range. At 2 nM insulin, this was true for up to 1 μM PIG, the total maximal effect approaching 130% of MIR under both conditions. Insulin (2 nM) combined with PIG concentrations above 1 μM provoked subadditive effects which did not exceed 160% of MIR. Taken together, the potentiating effects of compound **41** or **37** and insulin at low concentrations on insulin and PIG action, respectively, as well as the subadditive effects of the PIG compounds and insulin at high concentrations suggest that the signaling pathways used by the synthetic PIG compounds and insulin have some signaling steps and components in common. These may include tyrosine phosphorylation of IRS-1, a key component of the insulin signal transduction cascade in insulin-sensitive mammalian tissues located immediately downstream of the insulin receptor (for recent reviews, see refs *65*, *66*), and all the subsequent events leading to activation of the glucose transport system (for a review, see ref *67*), and the key metabolic enzymes, GS and GPAT.

To test this possibility, we studied the tyrosine phosphorylation state of IRS-1 in isolated diaphragms from normal rats after exposure to PIG compounds at about half-maximal and maximal effective concentrations with respect to stimulation of glucose transport and glycogenesis (see Tables 1 and 2). Total cellular IRS-1 was immunoprecipitated with anti-IRS-1 antibodies from the defatted supernatant of the homogenized and solubilized diaphragms and subsequently immunoblotted with anti-phosphotyrosine antibodies to identify tyrosine-phosphorylated IRS-1 or, alternatively, with anti-IRS-1 antibodies to demonstrate the amount of immunoprecipitated IRS-1. The autoradiogram (Figure 8) demonstrates that compounds **41**, **37**, **45**, and **7** induced tyrosine phosphorylation of IRS-1 in a concentration-dependent fashion (upper section). When corrected for the amounts of IRS-1 recovered with each immunoprecipitated sample, which actually differed to a minor degree, only (see lower section), compounds **41**, **37**, **45**, and **7** approached up to 95%, 65%, 55%, and 30% (at 10 μM) of MIR (at 100 nM) in inducing tyrosine phosphorylation of IRS-1. Taken together (this study and ref *15*), in isolated rat adipocytes, cardiomyocytes, and diaphragms, there is a strict correlation between the ability of PIG compounds to stimulate tyrosine phosphorylation of IRS-1 and to activate glucose transport and glucose metabolizing enzymes/pathways. Additional experiments demonstrated that the ability of the PIG compounds to trigger tyrosine phosphorylation of IRS-1 in diaphragms from Zucker fatty rats was not significantly impaired compared to that in diaphragms from normal rats (data not shown). Thus, induction of IRS-1 tyrosine phosphorylation by PIG compounds may form the molecular basis

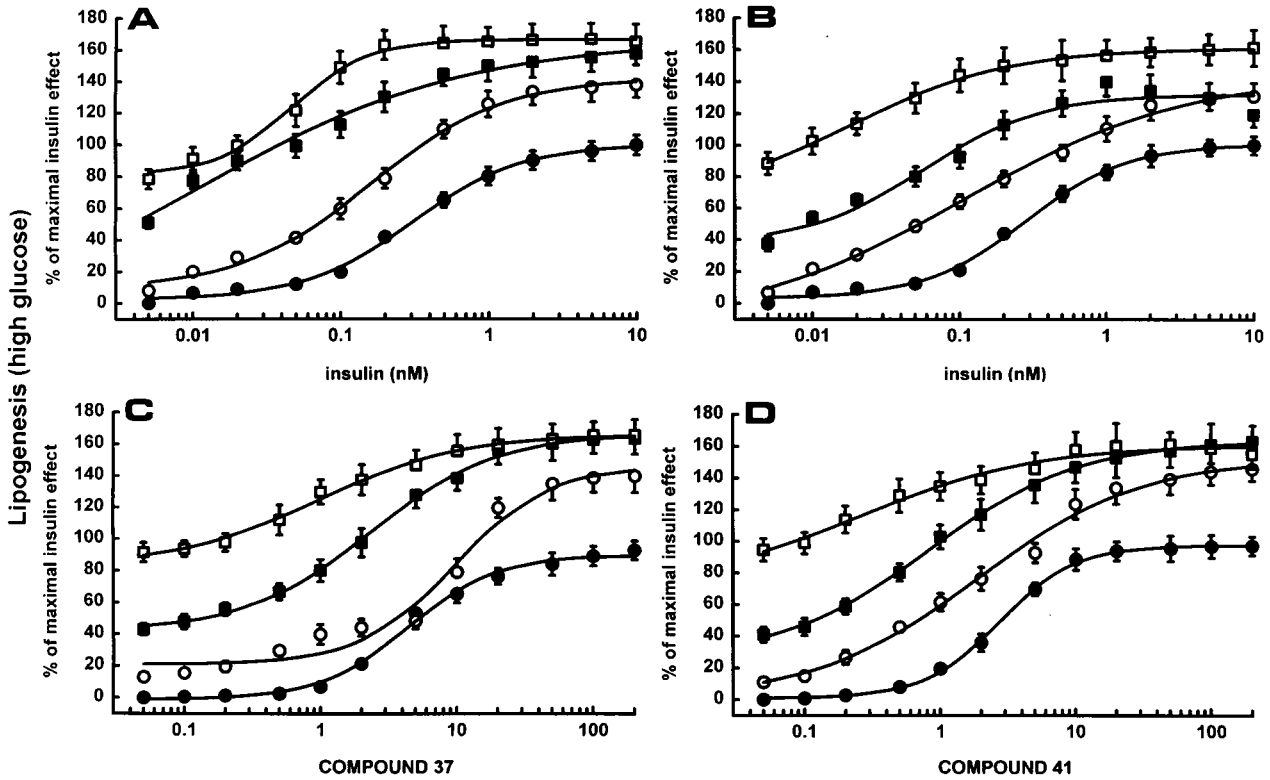

FIGURE 7: Effect of insulin on the insulin-mimetic activity of compounds **41** and **37**. Isolated rat adipocytes were incubated in the absence (closed circles) or presence of 0.5 (open circles), 2 (closed squares), and 20 μM (open squares) compound **37** (A) or **41** (B) with increasing concentrations of human insulin or, alternatively, in the absence (closed circles) or presence of 0.05 (open circles), 0.2 (closed squares), and 2 nM (open squares) insulin with increasing concentrations of compound **37** (C) or **41** (D) for 20 min at 37 °C. Subsequently, the cells were assayed for lipogenesis at high glucose. The insulin-mimetic activity was calculated as percent of the maximal stimulation factor provoked by 10 nM insulin alone which was 5.5-fold corresponding to 3.5 nmol of glucose incorporated into lipids per 3.5×10^5 cells and 90 min.

for their capability to bypass insulin resistance of nonoxidative glucose metabolism in muscle and adipose tissue provided the putative insulin resistance block is located upstream of IRS-1 as may be the case in the cellular models of insulin resistance used in the present study. The detailed characterization of the signaling pathway leading from the IRS proteins to the terminal effector systems used by the synthetic PIG compounds is the subject of current intensive investigation (W. Frick, J. Bauer, A. Bauer, S. Wied, G. Müller, in preparation).

During the initial period of the discovery of PIG molecules as insulin-mimetic compounds, it has been speculated that following generation by insulin-induced lipolytic cleavage of GPI lipids or membrane protein anchors at the outer or inner face of the plasma membrane of insulin-sensitive cells, these molecules bind directly to regulatory proteins (e.g., phosphatases) or enzymes (e.g., pyruvate dehydrogenase) of glucose and lipid metabolism thereby allosterically affecting their activity in an insulin-like manner. Although there is some experimental evidence for the insulin-dependent cleavage of GPI structures, leading to polar headgroups which exert partial insulin-mimetic activity in various cell-free and cell-based assay systems (for recent reviews, see refs *9*, *68*), definite proof for the existence of soluble intracellular mediators of (metabolic) insulin action is still missing.

Previously we demonstrated that the (potent) insulin-mimetic activity of the PIG-P from yeast in isolated rat adipocytes strictly depends on the presence of a trypsin/salt- and *N*-ethylmaleimide-sensitive protein at the outer face of the plasma membrane (*69*). Competition experiments with untreated adipocytes incubated in the presence of excess of the trypsinized soluble fragment of this protein strongly argued for a function of this protein as a receptor for PIG-P (*69*). This putative receptor may initiate the PIG signaling pathway which is coupled via downstream-located elements to the insulin signaling cascade; the point of interference may represent tyrosine phosphorylation of IRS-1. Currently we are studying whether the synthetic PIG compounds studied here also use this putative receptor protein. The demonstration of a direct interaction of radiolabeled synthetic PIG compounds with this protein would facilitate its identification.

CONCLUSIONS

Taken together, the synthetic PIG compounds presented here are capable of mimicking insulin action on major pathways of lipid and glycogen synthesis (stimulation of GS, GPAT, glucose transport, glycogenesis; inhibition of lipolysis) in four cellular models of insulin resistance: (i) adipocytes lacking a functional insulin receptor, (ii) adipocytes desensitized for insulin action by long-term incubation with high glucose and insulin, (iii) adipocytes from Zucker fatty rats, and (iv) diaphragms from Zucker fatty rats. Cellular insulin resistance can be caused by defects at each level of the signal-transmitting chain. At the level of insulin binding to its receptor, there is no evidence for a significant reduction of the number of functional receptors or of the insulin binding affinity in muscle and adipose tissues of type II diabetic patients (e.g., ref *70*). At the level of the receptor kinase itself, a number of defects or inactive states have been found in several cellular and animal models of insulin

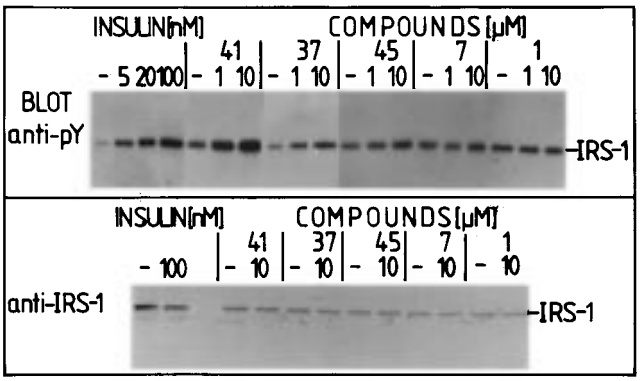

FIGURE 8: Effects of compounds **41**, **37**, **45**, **7**, and **1** on IRS-1 tyrosine phosphorylation in diaphragms. Isolated diaphragms from Wistar rats were incubated in the absence or presence of increasing concentrations of human insulin or compounds **41**, **37**, **45**, **7**, and **1**. Total homogenate proteins were subjected to immunoprecipitation with anti-IRS-1 antibodies and protein A/G-Sepharose as described in Materials and Methods. Subsequently, portions of the immunoprecipitates were immunoblotted with anti-phosphotyrosine antibodies (upper section) or anti-IRS-1 antibodies (lower section) using [^{125}I]protein A. An autoradiogram from a typical experiment is shown twice repeated with similar results. The identity of the radiolabeled polypeptide bands contained in the immunoprecipitates with IRS-1 was confirmed by stripping off (with high salt) the anti-phosphotyrosine antibodies from the blot (upper section) and subsequent re-immunoblotting with anti-IRS-1 antibodies. On both blots the position of the radiolabeled bands was identical corresponding to an apparent molecular weight of 170−185 kDa (data not shown). In additional control experiments, the use of nonimmune IgG instead of anti-IRS-1 antibodies did not result in immunoprecipitation of any phosphotyrosine-containing polypeptides or IRS-1 (data not shown).

resistance (e.g., ref *71*−*73*). Moreover, a kinase defect or inactivity in the skeletal muscle of type II diabetic patients and insulin-resistant Pima indians compared to nonobese control subjects was concluded from the observed rightward shift of the insulin concentration−response curve and the 50% reduction of the maximal autophosphorylation (*74*−*80*). A number of modulator systems have been identified which control the insulin receptor kinase activity (for a review, see ref *81*). An increase in inhibitory modulators might be an important mechanism causing insulin resistance through an inactive insulin receptor kinase. According to the structure−activity relationship derived from the present study, the synthetic PIG compounds interact with high potency and specificity with an as yet unidentified signaling machinery of rat adipocytes and diaphragms, which does not involve the insulin receptor kinase, and may therefore be helpful for finding a strategy to induce insulin-mimetic signaling in insulin-resistant cells.

REFERENCES

1. Bogardus, C. (1996) in *Diabetes Mellitus, Metabolic Abnormalities in the Development of Non-Insulin-Dependent Diabetes Mellitus* (LeRoith, D., Taylor, S. I., Olefsky, J. M., Eds.) pp 459−466, Lippincott-Reaven Publishers, Philadelphia, New York.
2. Reaven, G. M. (1996) in *Diabetes Mellitus, Insulin Resistance and Its Consequence: Non-Insulin-Dependent Diabetes Mellitus and Coronary Heart Disease* (LeRoith, D., Taylor, S. I., Olefsky, J. M., Eds.) pp 509−518, Lippincott-Reaven Publishers, Philadelphia, New York.
3. Baldini, G., Hohman, R., Charron, M. J., and Lodish, H. F. (1991) *J. Biol. Chem. 266*, 4037−4040.
4. Corvera, S., Jaspers, S., and Pasceri, M. (1991) *J. Biol. Chem. 266*, 9271−9271.
5. Robinson, L. J., Pang, S., Harris, D. S., Heuser, J., and James, D. E. (1992) *J. Cell Biol. 117*, 1181−1196.
6. Wheeler, T. J., Fell, R. D., and Hauck, M. A. (1994) *Biochim. Biophys. Acta 1196*, 191−200.
7. Tsakiridis, T., Vranic, M., and Klip, A. (1995) *Biochem. J. 309*, 1−5.
8. Chen, D., Elmendorf, J. S., Olson, A. L., Li, X., Earp, H. S., and Pessin, J. E. (1997) *J. Biol. Chem. 272*, 27401−27410.
9. Varela-Nieto, I., Leon, Y., and Caro, H. N. (1996) *Comp. Biochem. Physiol. 115B*, 223−241.
10. Müller, G., Schubert, K., Fiedler, F., and Bandlow, W. (1992) *J. Biol. Chem. 267*, 25337−25346.
11. Müller, G., Gross, E., Wied, S., and Bandlow, W. (1996) *Mol. Cell. Biol. 16*, 442−456.
12. Müller, G., Wied, S., Crecelius, A., Kessler, A., and Eckel, J. (1997) *Endocrinology 8*, 3459−3475.
13. Müller, G., Dearey, E.-A., and Pünter, J. (1993) *Biochem. J. 289*, 509−521.
14. Müller, G., Dearey, E.-A., Korndörfer, A., and Bandlow, W. (1994) *J. Cell Biol. 126*, 1267−1276.
15. Kessler, A., Müller, G., Wied, S., Crecelius, A., and Eckel, J. (1998) *Biochem. J. 330*, 277−286.
16. Cross, G. A. M. (1990) *Annu. Rev. Cell Biol. 6*, 1−39.
17. McConville, M. J., and Ferguson, M. A. J. (1993) *Biochem. J. 294*, 305−324.
18. Nosjean, O., Briolay, A., and Roux, B. (1997) *Biochim. Biophys. Acta 1331*, 153−186.
19. Murakata, C., and Ogawa, T. (1990) *Tetrahedron Lett. 31*, 2439−2442.
20. Murakata, C., and Ogawa, T. (1991) *Tetrahedron Lett. 32*, 101−104.
21. Murakata, C., and Ogawa, T. (1991) *Tetrahedron Lett. 32*, 671−674.
22. Murakata, C., and Ogawa, T. (1992) *Carbohydr. Res. 234*, 75−91.
23. Murakata, C., and Ogawa, T. (1992) *Carbohydr. Res. 235*, 95−114.
24. Ley, S. V., and Young, L. L. (1992) *Synlett 997*.
25. Zapata, A., and Martin-Lomas, M. (1992) *Carbohydr. Res. 234*, 93−106.
26. Frantova, A. Y., Stepanov, A. E., Bushnev, A. S., Zvonkova, E. N., and Sleets, V. I. (1992) *Tetrahedron Lett. 33*, 3539−3541.
27. Boons, G. J., Grice, P., Leslie, R., Ley, S. V., and Young, L. L. (1993) *Tetrahedron Lett. 84*, 8523−8526.
28. Khiar, N., and Martin-Lomas, M. (1995) *J. Org. Chem. 60*, 7071−7021.
29. Roberts, C., Madsen, R., and Fraser-Reid, B. (1995) *J. Am. Chem. Soc. 117*, 1546−1553.
30. Mootoo, D. R., Konradsson, P., and Fraser-Reid, B. (1989) *J. Am. Chem. Soc. 111*, 8540−8542.
31. Fraser-Reid, B., Udodong, U. E., Wu, Z., Ottosson, H., Merritt, J. R., Rao, C. S., Roberts, C., and Madsen, R. (1992) *Synlett 927*.
32. Kratzer, B., Mayer, T. G., and Schmidt, R. R. (1993) *Tetrahedron Lett. 34*, 6881−6884.
33. Udodong, U. E., Madsen, R., Roberts, C., and Fraser-Reid, B. (1993) *J. Am. Chem. Soc. 115*, 7886−7887.
34. Burfoot, M. S., Rogers, N. C., Watling, D., Smith, J. M., Pons, S., Paonessaw, G., Campbell, A. S., and Fraser-Reid, B. (1995) *J. Am. Chem. Soc. 117*, 10387−10388.
35. Madsen, R., Udodong, U. E., Roberts, C., Mootoo, D. R., Konradsson, P., and Fraser-Reid, B. (1995) *J. Am. Chem. Soc. 117*, 1554−1565.
36. Mayer, T. G., Kratzer, B., and Schmidt, R. R. (1994) *Angew. Chem. 106*, 2289−2293.
37. Mayer, T. G., Kratzer, B., and Schmidt, R. R. (1994) *Angew. Chem., Int. Ed. Engl. 33*, 2177−2180.
38. Fonteles, M. C., Huang, L. C., and Larner, J. (1996) *Diabetologia 39*, 731−734.
39. Cobb, J. E., and Johnson, M. R. (1991) *Tetrahedron Lett. 47*, 21−30.

40. Berlin, W. K., Zhang, W.-S., and Shen, T. Y. (1991) *Tetrahedron Lett. 47*, 1−20.
41. Caro, H.-N., Martin-Lomas, M., and Bernabe, M. (1993) *Carbohydr. Res. 240*, 119−131.
42. Zapata, A., Leon, Y., Mato, J. M., Varela-Nieto, I., Penades, S., and Martin-Lomas, M. (1994) *Carbohydr. Res. 264*, 21−31.
43. Plourde, R., d'Alarcao, M., and Saltiel, A. R. (1992) *J. Org. Chem. 57*, 2606−2610.
44. Termin, A., and Schmidt, R. R. (1989) *Liebigs Ann. Chem.* 789−795.
45. Aneja, R., Aneja, S. G., and Parra, A. (1995) *Tetrahedron Asymmetry 6*, 17−18.
46. Elie, C. J. J., Verduyn, R., Dreef, C. E., Braunts, D. M., van der Marel, G. A., and van Boom, J. H. (1990) *Tetrahedron 46*, 8243−8254.
47. Moody, A. J., Stan, M. A., and Stan, M. (1974) *Horm. Metab. Res. 6*, 12−16.
48. Müller, G., Ertl, J., Gerl, M., and Preibisch, G. (1997) *J. Biol. Chem. 272*, 10585−10593.
49. Müller, G., and Wied, S. (1993) *Diabetes 42*, 1852−1867.
50. Vila, M. C., Milligan, G., Standaert, M. L., and Farese, R. V. (1990) *Biochemistry 29*, 8735−8740.
51. Müller, G., Wied, S., Wetekam, E.-M., Crecelius, A., Unkelbach, A., and Pünter, J. (1994) *Biochem. Pharmacol. 58*, 985−996.
52. Guinovart, J. J., Salavert, A., Massague, J., Ciudad, C. J., Salsas, E., and Itarte, E. (1979) *FEBS Lett. 106*, 284−288.
53. Karnieli, E., Zarnowski, M. J., Hissin, P. J., Simpson, J. A., Salans, L. B., and Cushman, S. W. (1981) *J. Biol. Chem. 256*, 4772−4777.
54. Lawrence, J. C., Jr., Hiken, J. F., and James, D. E. (1990) *J. Biol. Chem. 265*, 19768−19776.
55. Honnor, R. C., Dhillon, G. S., and Londos, C. (1985) *J. Biol. Chem. 260*, 15122−15129.
56. Müller, G., Rouveyre, N., Upshon, C., and Bandlow, W. (1998) *Biochemistry 37*, 8705−8713.
57. Roussel, R., Carlier, P. G., Robert, J.-J., Velho, G., and Bloch, G. (1998) *Proc. Natl. Acad. Sci. U.S.A. 95*, 1313−1318.
58. Rhea, S., and James, D. E. (1997) *Diabetes 46*, 1667−1677.
59. Satoh, S., Nishimura, H., Clark, A. E., Kozka, I. J., Vannucci, S. J., Simpson, I. A., Quon, M. J., Cushman, S. W., and Holman, G. D. (1993) *J. Biol. Chem. 268*, 17820−17829.
60. Vannucci, S. J., Nishimura, H., Satoh, S., Cushman, S. W., Holman, G. D., and Simpson, I. A. (1992) *Biochem. J. 288*, 325−330.
61. Clarke, J. F., Young, P. W., Yonezawa, K. Kasuga, M., and Holman, G. D. (1994) *Biochem. J. 300*, 631−635.
62. Smith, O. L. K., and Czech, M. P. (1983) *Metabolism 32*, 597−602.
63. Terretaz, J., and Jeanrenaud, B. (1983) *Endocrinology 112*, 1346−1351.
64. Penicaud, L., Issad, T., and Ferre, P. (1988) in *Lessons From Animal Diabetes II* (Shafrir, E., Renold, A. E., Eds.) pp 438−443, J. Libbey, London, U.K.
65. White, M. F. (1997) *Diabetologia 40*, S2−S17.
66. Myers, M. G., Sun, X. J, and White, M. F. (1994) *Trends Biochem. Sci. 19*, 289−293.
67. Holman, G. D., and Kasuga, M. (1997) *Diabetologia 40*, 991−1003.
68. Stralfors, P. (1997) *BioEssay 19*, 327−336.
69. Müller, G., Wied, S., Piossek, C., Bauer, A., Bauer, J., and Frick, W. (1998) *Mol. Med. 4*, 299−323.
70. Grunberger, G., Zick, Y., and Gordon, P. H. (1984) *Science 223*, 932−934.
71. Debant, A., Guerre-Millo, M., LeMarchand-Brustel, Y., Freychet, P., Lavar, M., and VanObberghen, E. (1987) *Am. J. Physiol. 252*, E273−278.
72. Kadowaki, T., Kasuga, M., Akanuma, Y., Ezaki, O., and Takaku, F. (1984) *J. Biol. Chem. 259*, 14208−14216. Burant, C. F., Trentelaar, M. K., and Buse, M. G. (1986) *J. Clin. Invest. 77*, 260−270.
73. LeMarchand, Y., Gremeany, T., and Ballotti, R. (1985) *Nature 315*, 676−679.
74. Gremeaux, T., Tanti, J. F., VanObberghen, E., and LeMarchand-Brustel, Y. (1987) *Biochimie 69*, 387−393.
75. Freidenberg, G. R., Henry, R. R., Klein, H. H., and Olefsky, J. M. (1987) *J. Clin. Invest. 79*, 240−250.
76. Freidenberg, G. R., Reichart, D., Olefsky, J. M., and Henry, R. R. (1988) *J. Clin. Invest. 82*, 1398−1406.
77. Arner, P., Pollare, T., Lithell, H., and Livingston, J. N. (1987) *Diabetologia 30*, 437−440.
78. Caro, J. F., Sinha, M. K., and Raju, S. J. (1987) *J. Clin. Invest. 79*, 1330−1337.
79. Obermaier-Kusser, B., White, M. F., Pongratz, D., Su, Z., Ermel, B., Mühlbacher, C., and Häring, H. U. (1989) *J. Biol. Chem. 264*, 9497−9504.
80. Bulangu, L. N., Ossowski, V. M., Bogardus, C., and Mott, D. (1990) *Am. J. Physiol. 258*, E964−974.
81. Häring, H. U. (1991) *Diabetologia 34*, 848−861.

BI9806201